



The
University
Of
Sheffield.

In the process of Raman activated cell sorting for single cell analysis

A Thesis Submitted to the University of Sheffield for the Degree
of Master of Philosophy

Di Zhu

Department of Civil and Structural Engineering

October 2014

Declaration

The author declares that this thesis is the presentation of author's own work and has not been submitted for any degree before. All sources from others have been clearly indicated and acknowledged.

Signature:

Date:

Acknowledgements

First and foremost, I would like to express my appreciation to my supervisor Dr. Wei Huang from University of Sheffield for his great contribution in single cell Raman microspectroscopy and kind supervision of this project. Wei is a talented and hard-working scientist, a pioneer in single cell Raman research. As a supervisor, he takes care of every student and is always glad to provide patient guidance. Without his comprehensive knowledge for academic research I couldn't complete this project. I also received frequent encouragement from Wei, which gave me the courage to conquer all difficulties throughout my study.

Also I gratefully acknowledge Prof. Neil Hunter and Michaël Cartron from University of Sheffield, Prof. Colin Murrell, Oliver Burns and Carolina Grob from University of East Anglia, Dr. Aliyu Ibrahim Dabai from Queen's University Belfast, Dr. Dayi Zhang from Lancaster University for providing samples, and all co-authors of published papers for their great work.

I would like to thank all staff in the Groundwater Protection and Restoration Group (GPRG) for their valuable help and support. I want to specially thank Dr. Paul Davison for kindly reviewing this thesis.

Further thanks are given to the University of Sheffield for financial support for my tuition fee, and my parents for their financial support for my living costs in Sheffield.

Abstract

The majority of microorganisms in nature are currently unculturable. However, increasing evidence shows that these uncultured microbes play important roles in ecosystem. Many culture-independent approaches (e.g. Metagenomics, stable isotope probing) have been developed to address this challenge. Among these approaches, single cell Raman microspectroscopy is a label-free, noninvasive technique that allows to do biochemical profile measurement at the single-cell level; on the other hand, it also enables to isolate individual cells using a new technique called Raman activated cell ejection (RACE).

This study aims to establish a whole system of single cell Raman analysis, which includes the single cell identification, isolation and single cell genomics. The Stable isotope probing (SIP) combined Raman technique also serves to link specific microbial species to their functions. In this study, several natural biomarkers were discovered to identify specific bacteria, including the single cell Raman signal of proteorhodopsin, which is the first time to be discovered at the single-cell level. The Raman-SIP technique was used to measure ^{13}C -labeled samples, in which a ^{13}C -labeled Magnetic nanoparticles (MNPs) free environmental sample was also involved and can be detected. More importantly, the Raman band of C-D stretching was firstly be discovered, which indicated that for the first time the deuterium-labeled bacteria can be detected by single cell Raman microspectroscopy. The RACE technique was proved functional and successfully ejected MNPs-free samples, and a positive result of single cell DNA amplification was carried out using *P. putida* UWC1 (GFP) cells.

This study had a contribution for the identification of some biomarkers from microbial species through their special Raman spectra, which paved the way for single cell ejection; it also broden the knowledge of Raman-SIP analysis by discovering significant shift of C-D Raman band. The RACE technique was developed and a successful single cell gene sequencing has

been proven, though the challenge of contamination remains unsettled yet. As a consequence, this study has strengthened single cell Raman analysis and laid the foundation for further development and applications of RACE.

List of publication

Article

1. Wang, Y., Song, Y., Zhu, D., Ji, Y., Wang, T., McIlvenna, D., Yin, H., Xu, J. & Huang, W.E. 2013. Probing and sorting single cells - the application of a Raman-activated cell sorter. *Spectroscopy Europe*, 25(5), 16-20.

Contributed Raman spectra of *E. coli* alkane production strain and the wide-type *E. coli* strain, as well as their comparison, indicated that single cell Raman measurement can be used in synthetic biology; the screenshot pictures before and after isolating a interested single cell using Raman-activated cell ejection (RACE) technique, as well as the single cell Raman spectra (SCRS) of unlabeled and ^{13}C -labeled individual cells, proved that RACE can successfully isolate the cell of interest. Those can be found in Figure 4-3 and Figure 2-3 (b) in this thesis.

Academic Papers

1. Zhang, D., Berry, J. P., Zhu, D., Wang, Y., Chen, Y., Jiang, B., Huang, S., Langford, H., Li, G., Davison, P. A., Xu, J., Aries, E. & Huang, W. E. 2014. Magnetic nanoparticle-mediated isolation of functional bacteria in a complex microbial community. *ISME J.* Online published. doi: 10.1038/ismej.2014.161

Contributed SCRS of an unlabeled single cell and a ^{13}C -labeled single cell from an environmental sample treated with Magnetic nanoparticles (MNPs), as well as their cell images. The result indicated that single cell Raman measurement enables to detect stable isotope labeled individual cells from environmental samples, and proved that most cells in the MNPs-free sample were successfully labeled with ^{13}C . The result can be found in Figure 4-15 in this thesis.

2. Jiang, B., Zhu, D., Song, Y., Zhang, D., Liu, Z., Zhang, X., Huang, W. E. & Li, G. 2014. Use of a whole-cell bioreporter, *Acinetobacter baylyi*, to estimate the genotoxicity and bioavailability of chromium (VI)-contaminated soils. *Biotechnology Letters*. Online published. doi: 10.1007/s10529-014-1674-3

Contributed the majority of data and the following analysis except Figure 1 in the above paper.

3. Berry, D., Mader, E., Lee, T. K., Woebken, D., Wang, Y., Zhu, D., Palatinszky, M., Schintlmeister, A., Schmid, M. C., Hanson, B. T., Shterzer, N., Mizrahi, I., Rauch, I., Decker, T., Bocklitz, T., Popp, J., Gibson, C. M., Fowler, P. W., Huang, W. E. & Wagner, M. 2015. Tracking heavy water (D₂O) incorporation for identifying and sorting active microbial cells. *Proceedings of the National Academy of Sciences*, 112, E194-E203.

Contributed SCRS of *E. coli* cells fed with different percentage of fully deuterium-labeled glucose. Because the above paper is focused on D₂O labeling, this figure was provided as a supplement, indicated that the C-D peak can be detected when cells were fed with other D-labeled substrates. This result can be found in Figure 4-20 in this thesis.

Table of contents

Declaration	i
Acknowledgements	ii
Abstract	iii
List of publication	v
Table of contents	vii
List of figures.....	ix
List of tables	xiii
Glossary	xiv
Chapter 1: Introduction	1
1.1 Introduction to unculturable microbes	1
1.2 Research aims and objectives	2
Chapter 2: Literature review: Current advances in the study of unculturable microorganisms	5
2.1 Metagenomics	5
2.2 Stable isotope probing	7
2.3 Single-cell techniques and FACS	8
2.4 Single cell Raman microspectroscopy	10
2.4.1 Introduction and basic theory of Raman microspectroscopy	10
2.4.2 Identification of microbial species, linking species to their functions	11
2.4.3 Isolation of single cells	14
2.5 Summary	18
Chapter 3: Materials and methods	20

Chapter 4: Results and discussion	28
4.1 Searching for natural biomarkers in SCRS	28
4.2 Raman-SIP measurement.....	42
4.2.1 Measurement of ¹³ C-labeled cells	42
4.2.2 Measurement of Deuterium-labeled cells	49
4.3 Multivariate data analysis of SCRS	55
4.4 Raman based Single cell isolation and gene sequencing	60
Chapter 5: Conclusion.....	63
Chapter 6: Proposed future works.....	64
References.....	66
Appendix.....	73

List of figures

- Figure 2-1.** A typical SCRS of *Acinetobacter baylyi* ADP1 using 532 nm laser (laser power: 35 mW, acquisition time: 10 s). (Huang *et al.*, 2010) 12
- Figure 2-2.** The red-shift SCRS comparison between ^{12}C and fully ^{13}C -labeled *E. coli* samples using 532 nm laser (laser power: 35 mW, acquisition time: 20 s). Each SCRS is the average result from 20 replicates. 14
- Figure 2-3.** (a) Schematic picture of the Raman activated cell ejection (RACE) technique. (b) Comparison of before and after the isolation of a single cell by RACE (50x zoom lens)..... 17
- Figure 4-1.** The averaged and normalized SCRS from 20 replicates of *Rhodobacter sp.* (acquisition time: 1s)..... 29
- Figure 4-2.** The averaged and normalized SCRS from 20 replicates of *Ralstonia eutropha* H16 (acquisition time: 30s)..... 30
- Figure 4-3.** The averaged and normalized SCRS from 20 replicates of alkane synthesizing *E. coli* samples and *E. coli* control sample (acquisition time: 20s)..... 31
- Figure 4-4.** Ratio of $2936.6\text{ cm}^{-1}/1003.6\text{ cm}^{-1}$ of averaged and normalized SCRS from 20 replicates of alkane synthesizing *E. coli* samples and *E. coli* control sample. 32
- Figure 4-5.** The averaged and normalized SCRS from 20 replicates of proteorhodopsin-expressing *E. coli* single cells (acquisition time: 120s)..... 34
- Figure 4-6.** The SCRS for rapid screening of a PR-containing *E. coli* single cell (acquisition time: 3s). 35

Figure 4-7. (a) The image of an <i>E. coli</i> MC1000 mini-cell (100× zoom lens). (b) A typical Raman spectrum of a PR-containing MC1000 mini-cell (acquisition time: 120s).	36
Figure 4-8. (a) PR formation of sample 4 in averaged and normalized SCRS at all the time points (acquisition time: 120s). (b) Comparison around 1536 cm ⁻¹ in averaged and normalized SCRS between 4 samples at t = 180 min (acquisition time: 120s).	38
Figure 4-9. Ratio – time dynamic curve of PR, calculated from 6 replicates in sample 4 at all 5 time points.	39
Figure 4-10. (a) Microscope image of the new <i>Micrococcus</i> strain (100× zoom lens). (b) The averaged and normalized SCRS from 20 replicates of the <i>Micrococcus</i> strains incubated in LB, MM and MM without NH ₄ Cl.	41
Figure 4-11. The averaged and normalized SCRS from 20 replicates of different ¹³ C-content labeled <i>Methylophaga marina</i> (acquisition time: 15s).	44
Figure 4-12. Calibration curve of 1622 cm ⁻¹ /1671 cm ⁻¹ ratio - ¹³ C content from <i>Methylophaga marina</i> SCRS. Calculated from 20 replicates in each sample.	45
Figure 4-13. The averaged and normalized SCRS from 20 replicates of different ¹³ C-content labeled <i>Methylomonas methanica</i> MC09 (acquisition time: 0.1s).	46
Figure 4-14. (a-c) Calibration curve of Raman peak wavenumber - ¹³ C content from <i>Methylomonas methanica</i> MC09 SCRS. Calculated from 20 replicates in each sample.	47
Figure 4-15. The normalized SCRS of unlabeled and ¹³ C-labeled MNPs-free single cells (acquisition time: 20s).	49

Figure 4-16. The averaged and normalized SCRS from 20 replicates of 100% D-labeled and unlabeled <i>Pseudomonas putida</i> G7 single cells (acquisition time: 20s).....	50
Figure 4-17. The Raman spectrum for rapid screening of a 100% D-labeled <i>Pseudomonas putida</i> G7 single cell (acquisition time: 4s).	51
Figure 4-18. The averaged and normalized SCRS from 30 replicates (10 individual cells × 3 biological replicates) of different D-content labeled <i>Pseudomonas putida</i> F1 (acquisition time: 20s).....	52
Figure 4-19. Calibration curve of D-percentage – 2182 cm ⁻¹ /baseline ratio from <i>Pseudomonas putida</i> F1 SCRS. Calculated from 30 replicates (10 individual cells × 3 biological replicates) in each sample.	53
Figure 4-20. (a) The averaged and normalized SCRS from 30 replicates (10 individual cells × 3 biological replicates) of different D-content labeled <i>Escherichia coli</i> cells (acquisition time: 20s). (b) The close view of phenylalanine peak in Figure 4-20 (a).	54
Figure 4-21. (a) The averaged and normalized Raman spectra from 9 replicates of 8 species (<i>Citrobacter</i> , <i>E. coli</i> , <i>Enterobacter</i> , <i>Enterococcus</i> , <i>Klebsiella</i> , <i>Pseudomonas</i> , <i>S. aureus</i> , <i>Streptococcus</i>). (b) The averaged and normalized Raman spectra from 9 replicates of 4 <i>Citrobacter</i> strains.	57
Figure 4-22. (a) DFA result of SCRS analysis from 8 species (<i>Citrobacter</i> , <i>E. coli</i> , <i>Enterobacter</i> , <i>Enterococcus</i> , <i>Klebsiella</i> , <i>Pseudomonas</i> , <i>S. aureus</i> , <i>Streptococcus</i>). (b) DFA result of SCRS analysis from 4 species (<i>Citrobacter</i> , <i>E. coli</i> , <i>Enterobacter</i> , <i>Klebsiella</i>).	59

Figure 4-23. Comparison images before and after isolation of a ^{13}C -labeled MNPs-free single cell by RACE (50x zoom lens). 60

Figure 4-24. The gel image of PCR genomic DNA from 8 samples. L is a 1Kb DNA marker ladder, 1-6 are the numbers of the samples, + + is the positive control, - - is the negative control..... 62

List of tables

Table 2-1. Comparison of different culture-independent techniques..	19
Table 3-1. List of strains used in this study and their growth conditions.	21
Table 4-1. Sample information of PR-expressed <i>E. coli</i>	33
Table 4-2. Sample information of PR-expressing <i>E. coli</i> cells used in dynamic analysis.	37
Table 4-3. Sample information for ¹³ C-labeled <i>Methylophaga marina</i>	43
Table 4-4. Sample information for ¹³ C-labeled <i>Methylomonas</i> <i>methanica</i> MC09.....	46
Table 4-5. 29 bacterial strains and their IDs in single cell Raman microspectroscopy measurement.	56

Glossary

DFA	Discriminant functional analysis
dH ₂ O	Distilled water
DNA	Deoxyribonucleic acid
dNTPs	Deoxynucleotide Triphosphates
EDTA	Ethylenediaminetetraacetic acid
FACS	Fluorescence activated cell sorting
FISH	Fluorescence <i>in situ</i> hybridization
GFP	Green fluorescent protein
laser	Light amplification by stimulated emission of radiation
LB	Luria-Bertani
LIFT	Laser-induced forward transfer
MAR	microautoradiography
MM	Minimal medium
MNPs	Magnetic nanoparticles
pABA	4-Aminobenzoic acid
PCA	Principal component analysis
PCR	Polymerase chain reaction
PR	Proteorhodopsin
RACE	Raman activated cell ejection

RNA	Ribonucleic acid
SCRS	Single cell Raman spectrum
SIP	Stable isotope probing
TAE	Tris-acetate-EDTA

Chapter 1: Introduction

1.1 Introduction to unculturable microbes

A variety of microorganisms can be found in almost every environmental habitat. They are the fundamental units of life and play an essential role in food, medicine, energy, water treatment, human health, etc. Ever since bacteria were first discovered in 1684, scientists have never stopped researching these smallest forms of life, and numerous achievements have been made to help people have a better understanding of the bacterial world.

Over the past 300 years, traditional molecular biology techniques have been highly dependent on microbial culturing, in which microorganisms are isolated from the environment, or other organisms, and incubated and grown in a culture media in the laboratory. Although significant progress has been made through the culturing of microbial species, as the knowledge of microbiology steadily increased, scientists gradually realized the astonishing fact that the majority of prokaryotes (probably more than 99%) are currently unculturable (Amann *et al.*, 1995). Undoubtedly, microbes in the environment are highly diverse and the lack of knowledge in dealing with unculturable microbes severely hampers our study of the microbial world and may sometimes narrow our view when researching samples *in situ*, because relying on culturing alone will definitely change the structure and composition of microbial communities. In fact, it has been proved that some unculturable microbial species play the most important role in biodegradation; for example, Huang and co-workers (Huang *et al.*, 2009a) have identified an unculturable *Acidovorax sp.* as the dominant degrader in naphthalene biodegradation in ecosystem instead of *Pseudomonas sp.*, which is a culturable bacteria and previously considered as the major degrader.

There are several possible reasons why the majority of microorganisms are currently unculturable. Some of them do have critical growth

requirements (nutrients, pH, temperature, etc.) (Kopke *et al.*, 2005) and are able to become culturable if the proper growing conditions can eventually be found. Some microbes can be inhibited when cultured in a mixture by bacteriocins released by other strains, or some unknown antibacterial substances in the medium (Tamaki *et al.*, 2005). In some other cases, cross-feeding or beneficial cooperation may exist between different species (Mikx and Vanderhoeven, 1975, Belenguer *et al.*, 2006), making them unable to be cultured individually. Cell-to-cell interactions are also considered to be responsible for cell growth through network signals that can control the microbial community structure and even the survival of microbial species (Whitehead *et al.*, 2001, De Kievit *et al.*, 2001). Unculturable microbes may become culturable if the correct growing media and proper conditions (temperature, pH, etc.) can be found, but this is time-consuming and can turn out to be inefficient when dealing with previously unaccounted species. Thus, various culture-independent techniques have been discovered and developed to help scientists look into the “dark side” of the molecular biological world, including metagenomics, stable isotope probing (SIP) and various single-cell techniques (for a review, see Chapter 2).

Single cell Raman microspectroscopy is a single-cell technique that has emerged in the past few years. Compared with other single-cell techniques, it is a noninvasive, label-free method to rapidly acquire biochemical information from individual cells *in situ*, represented as single cell Raman spectra (SCRS) containing over 1000 bands that provide rich profiles of a single cell. It also provides a powerful tool for the isolation of interesting single cells when used in conjunction with Raman-tweezers and Raman activated cell ejection (RACE). When combined with fluorescence in situ hybridization (FISH) and SIP (Huang *et al.*, 2007b, Huang *et al.*, 2009a), this powerful approach can provide even more research opportunities. A detailed introduction to single cell Raman microspectroscopy is given in section 2.4.

1.2 Research aims and objectives

This study aims to establish a complete system to successfully identify and isolate single cells from environmental communities, do single cell DNA amplification and gene sequencing, also link specific species to their functions using SIP-associated single cell Raman microspectroscopy technique.

The objectives of this project are:

(1) Find special bands in SCRS as biomarkers to identify and differentiate specific microbial species, as well as to link these species to functional attributes using SIP. In this project, besides researching the reported signals, new biomarkers and stable-isotopes will also be explored.

(2) Develop the Raman activated cell ejection (RACE) technique, optimize the operating conditions, and establish the whole system of single cell identification, isolation and single-cell genomics.

(3) Gain a comprehensive understanding of the attributes of unculturable microorganisms using single-cell Raman technique. It includes the phenotype of specific microbial species (e.g. physiological properties, biochemical information), which can be observed using Raman measurement; their functional attributes in ecosystem, which can be analyzed using Raman-SIP; and their genotype, which can be acquired using single-cell gene sequencing towards isolated cells.

In this thesis, a literature review is in Chapter 2 that gives an introduction to some common culture-independent approaches (Metagenomics, stable isotope probing, fluorescence activated cell sorting, and single cell Raman microspectroscopy), and a summary to their advantages along with disadvantages. Chapter 3 describes materials and methods that were used in this study, including sample preparation, measurement and analysis. Chapter 4 presents and discusses results that have done in MPhil period: several biomarkers and SIP-associated cells have been measured, including a new biomarker and stable isotope detection that

haven't previously been reported in bacteria; the single cell isolation and gene amplification has begun to be tested and proved to be workable, although some challenges remain to be solved. Chapter 5 is a conclusion of this study and Chapter 6 gives a suggestion of potential future works of single cell Raman research.

Chapter 2: Literature review: Current advances in the study of unculturable microorganisms

In order to investigate the mysterious world of unculturable microorganisms, many culture-independent techniques, which means the techniques that can be used in microbial study without a pure cultivation in laboratory, have been invented, aiming to find out what these microbes are, how they behave and influence the environment, and harvest their genes to increase our knowledge of the molecular biological world. Originally, several population-levelled techniques were developed and found to be effective and were commonly used in the research of unculturable microbes, such as metagenomics and stable isotope probing. However, with the continued deepening of research, scientists were no longer satisfied with just observing the average status of microbial communities rather than the individual cells themselves. More importantly, some drawbacks inherent in these techniques prompted scientists to establish more efficient tools and hence more and more different single-cell techniques were developed. Traditional single-cell techniques, for example fluorescence activated cell sorting (FACS), effectively solved the problem of isolating individual cells, but has been criticized due to several shortcomings. Amongst the many single-cell techniques now available, single cell Raman microspectroscopy is an emerging but promising one. It is a noninvasive, label-free treatment and the unique functions of the laser provide researchers with more freedom to study single cells.

2.1 Metagenomics

Metagenomics, first mentioned by Handelsman and co-workers in 1998 (Handelsman et al., 1998), is one of the most common and effective culture-independent methods for genomic analysis of microbial communities. Metagenomics enables complete genes to be directly extracted from complex environmental microbial communities without using cultivation methods. To do this, the DNA of microbial communities from environmental samples was

extracted and cloned into a vector; clones were then transformed into a culturable host bacterium (e.g., *E. coli*), and researchers can screen the resulting transformants using “anchors” (Handelsman, 2004). The trouble of cultivation can therefore be avoided. Analysis can be divided into sequence-driven analysis and function-driven analysis. Sequence-driven analysis allows complete gene sequences to be screened for and harvested by identifying phylogenetic anchors, whilst function-driven analysis enables to identify genes that express a function, regardless of whether or not the gene was recognized via sequence analysis in advance. These features provide researchers with a way collect various gene fragments within one microbial group, do random sequencing on mixed environmental microbial samples, and identify new functional genes. Metagenomics has been widely used and has generated numerous achievements. For instance, researchers have successfully acquired genes from uncultured microbes in the northwest Sargasso Sea (Venter et al., 2004) through whole-genome shotgun sequencing and from acid mine drainage (Tyson et al., 2004). Countless new antibiotics and enzymes have also been discovered using this technique.

However, culture-independent as this method is, many researchers decided to extract DNA after pre-cultivation in the laboratory because of the practical difficulties involved in directly extracting the whole DNA from environmental samples (Streit *et al.*, 2004, Tsai and Olson, 1992). There are also several other drawbacks that limit the power of this approach. For example, sequence-driven analysis is highly reliant on already available databases containing full genomic sequences in order to understand the information in the gene sequences (Streit *et al.*, 2004). The phylogenetic markers used in screening also restrict the study, because the genome of interest must already contain the available markers, and thus scientists need to enlarge the collection of markers that can be used. Also, the low speed and expensive cost make it impractical to sequence a large amount of complex samples from the environment. Most importantly, metagenomics is limited in its ability to link specific species to their functions, because most of the functional genes may not be expressed in a particular host bacterium

(Handelsman, 2004). Although many techniques are increasingly being added to improve metagenomics, new methods are still required to deepen our understanding of unculturable microbes.

2.2 Stable isotope probing

Stable isotope probing (SIP) is an approach for researching unculturable microorganisms that has rapidly developed in recent years. The traditional isotope labelling technique involves incubating samples with a special substrate labeled with an isotope, so that those microbial species who use this substrate to support their growth will become labeled with this isotope. The labeled isotope can be used as a “tracker” for researchers to find out, for example, how ecosystems work and what kind of role the target microorganisms play. Based on this principle, scientists have successfully combined fluorescence *in situ* hybridization (FISH) with microautoradiography (MAR) as FISH-MAR (Lee *et al.*, 1999, Ouverney and Fuhrman, 1999, Daims *et al.*, 2001), a tool to determine which microorganisms in the environment use the radioactive isotope labeled substrate as a metabolite (by MAR) and to then identify these microbes (by FISH).

Stable isotope probing (SIP) was established by Radajewski and co-workers in 2000 (Radajewski *et al.*, 2000). The substrate used in this technique is labeled with a heavy but non-radioactive isotope, which makes this method safer and easier to operate when compared with radioactive isotope. The labeled DNA will be slightly heavier than the normal DNA and can be clearly separated and isolated using density gradient centrifugation (Neufeld *et al.*, 2007) for subsequent use in genomic analysis. Manefield and co-workers developed RNA-SIP in 2002 (Manefield *et al.*, 2002a, Manefield *et al.*, 2002b), making this method even more comprehensive. In most cases, researchers use ^{13}C -labeled substrate as a carbon source; a typical example can be found in the experiments of Boschker and co-workers, who used ^{13}C -labeled acetate and methane in the study of sulphate reduction and methane

oxidation (Boschker *et al.*, 1998). ^{15}N (Cadisch *et al.*, 2005, Buckley *et al.*, 2007) and ^{18}O (Schwartz, 2007) has also been shown to be usable isotopes.

SIP is a safe and convenient approach and is still one of the most common tools used for the study of unculturable microorganisms at present. The isotope probing treatment gives the ability to link microbial species to their biochemical functions in a culture-independent way. However, like many other techniques, SIP has its own inherent weaknesses. Due to its unique methodology, SIP always exerts a destructive effect on the microorganisms whilst the laboratory pre-treatment destroys any information about the location and distribution of particular microbial species in complicated environmental samples. Therefore, it fails to give us information about the phenotype of microbial species and their conditions *in situ*. Moreover, the results of SIP can only be based on large amount of cells, which is, of course, the limitation also inherent in all previous population-leveled techniques.

In recent years, with the development of culture-independent techniques, researchers found that SIP could be more powerful when combined with other approaches. Huang and co-workers (Huang *et al.*, 2004, Huang *et al.*, 2007b, Huang *et al.*, 2009a) combined DNA-SIP with Raman microspectroscopy and found “red-shift” bands in cells labeled with ^{13}C and ^{15}N , pushing this method to the single-cell level (for the details of Raman-SIP technology, see section 2.4.2). Further advanced applications of SIP in the future will definitely prove to be very promising.

2.3 Single-cell techniques and FACS

Population-leveled techniques, no matter how advanced they have become, always reflect the average situation of multiple cells. Single-cell techniques, however, enables to present information about individual cells in microbial communities. Due to cellular heterogeneity, cell-to-cell variations are shown not only in varying gene expression, but also in physiological processes, phenotypes, and so forth (Brehm-Stecher and Johnson, 2004,

Kaern et al., 2005, Avery, 2006). Hence, single-cell techniques provide a comprehensive understanding of microbial functions and activities in a culture-independent way *in situ*. More and more new methods have been successfully applied and developed focusing on identification and isolation of single cells, involving fluorescence *in situ* hybridization (FISH), green fluorescent protein (GFP), various types of cytometry and electrorotation (Brehm-Stecher and Johnson, 2004).

Among different types of single-cell techniques, fluorescence activated cell sorting (FACS) (Herzenberg *et al.*, 1976) is considered to be one of the leading approaches to isolate cells according to fluorescent signals from individual cells (Herzenberg et al., 2002, Brehm-Stecher and Johnson, 2004). FACS, as a type of flow cytometry, provides an approach to sort mixed microbial communities into two or more containers, one cell at a time, using a special light source (e.g. laser) and fluorescent labelling. Individual cells in liquid media firstly flow through a measuring station where data on light scattering and fluorescence characterization is recorded. The Drops containing the cell are given an electronic charge depending on the fluorescence dye of the cell, and can be divided into different containers when flowing through an electrostatic deflection system. Therefore, researchers are able to collect cells of interest at the single-cell level, as well as collect information about cell size, shape, number and the content in communities.

FACS has proved to be a fast and objective way to isolate particular single cells and can collect information about their phenotype, but there are several drawbacks that cannot be ignored. First of all, like any other fluorescence-based techniques, *a priori* knowledge is required about what DNA/RNA sequence or protein in the cell can be a target. Secondly, cells should be suspended in aqueous media, which may not be easy to do when using soil, sludge or tissues samples, as some cells may be encapsulated in a slime layer or extracellular matrix. Thirdly, the invasive staining step usually makes the cells unable to survive following cell sorting, making it difficult to culture the sorted cells. Lastly, fluorescence can only be determined by either

it is presence or absence. As a result, FACS is not a perfect approach to extensively resolve the problem of investigating unculturable microorganisms.

2.4 Single cell Raman microspectroscopy

2.4.1 Introduction and basic theory of Raman microspectroscopy

The Raman effect, which is the inelastic scattering of photons from the sample, was first discovered experimentally by C. V. Raman and Krishnan in 1928 (Raman and Krishnan, 1928). Since then, this phenomenon has been referred to as Raman spectroscopy. In Raman scattering (Browne and McGarvey, 2007, Huang *et al.*, 2010, Long, 2002, Smith and Dent, 2005), when impinging a monochromatic light source on a sample, the light has an interaction with the molecule and forms a unique and short-lived state called the “virtual state”, which is different from Rayleigh scattering. This state is unstable and absorbed photons will be quickly re-radiated, leading to 2 possible results. If the energy is transmitted from the incident photon to the molecule, the scattered light will contain a lower energy and frequency (or longer wavelength) than the incident light, which is called Stokes scattering. However, if the energy is transmitted from the molecule to the incident photon, the scattered light will contain a higher energy and frequency (or shorter wavelength), which is called anti-Stokes scattering. In either case, the energy difference between the incident photon and the inelastically scattered photon will result in a particular intensity that will vary from each other. Generally, Stokes scattering is much stronger than anti-Stokes scattering and intensities caused by Stokes scattering are eventually present in a Raman spectrum.

Raman microspectroscopy, first mentioned by Puppels and co-workers in 1990 (Puppels *et al.*, 1990), is the technique that combines Raman microspectroscopy with optical microscopy. This new technique allows researchers to focus the monochromatic laser as a light source on one single cell (Huang *et al.*, 2004) and acquire the Raman signal from its biochemical

profile. In addition, the laser can also create a single-beam gradient force trap and capture the interested single cell in aqueous media (Xie and Li, 2003, Xie *et al.*, 2005a, Huang *et al.*, 2004). In the last two decades, researchers have paid increasing attention to this technique and shown it to be a noninvasive, powerful and efficient tool to identify different microbial species, link species and distribution with functions, and isolate interested single cells, all without any pre-treatment. Other more specific applications can also be created when combining single cell Raman microspectroscopy with other tools (e.g. SIP, FISH, etc.).

2.4.2 Identification of microbial species, linking species to their functions

In order to have a better understanding of microorganisms, it is essential that single cell techniques should first be able to identify different microbial species within environmental samples rapidly. Single cell Raman microspectroscopy provides a noninvasive, label-free way to harvest information-rich biochemical profiles of individual cells. A typical single cell Raman spectrum (SCRS) contains over 1000 bands, mainly within the range of 500-2000 cm^{-1} (for an example, see Figure 2-1). Those bands work as a “fingerprint” to offer information about numerous biochemical compounds e.g. carbohydrate, proteins, polysaccharides, and lipids (for more information about Raman bands, see Appendix 1). Harvesting these signals doesn't require any labelling (Huang *et al.*, 2010), making this method one of the best approaches to study the physiology of cells. Moreover, the acquisition time to get a good SCRS is fairly short (usually 1-20s) for bacteria, and if some specific “markers” can be found, such as carotenoid pigments, the acquisition time can be shortened to 0.1-1s. Such features make it an extremely useful and efficient tool to enable direct phenotypical identifications of single cells.

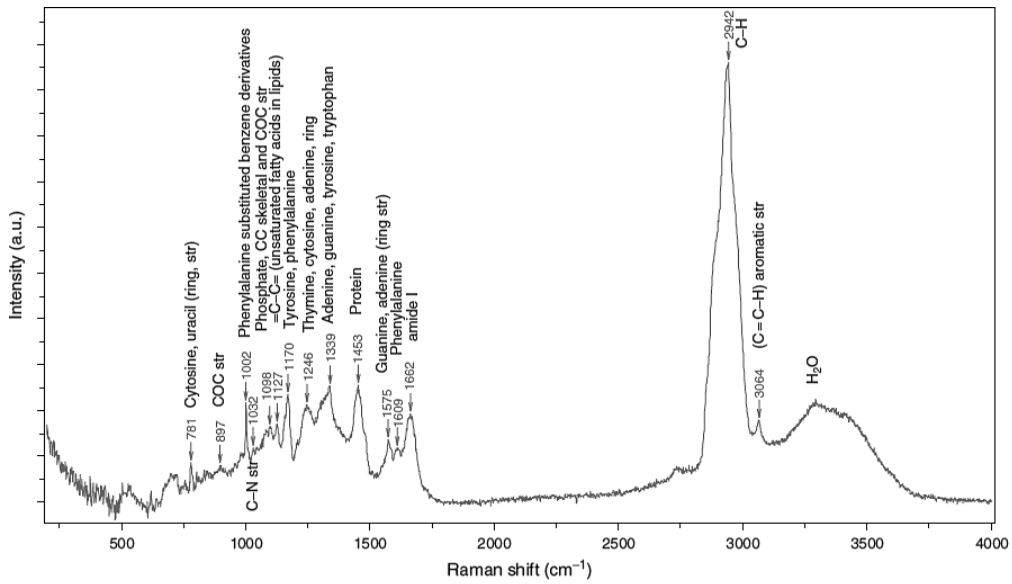


Figure 2-1. A typical SCRS of *Acinetobacter baylyi* ADP1 using 532 nm laser (laser power: 35 mW, acquisition time: 10 s). (Huang *et al.*, 2010)

Raman microspectroscopy can not only express the condition of phenotypes from single cells, but is also be a sensitive tool to distinguish between different species, as well as different strains within a species, through the slight distinctions and differences seen between various spectra. Researchers have published many articles proving that Raman spectroscopy is able to classify different bacterial species both at the population level (Goodacre *et al.*, 1998, Choo-Smith *et al.*, 2001, Maquelin *et al.*, 2000, Maquelin *et al.*, 2002a) and the single-cell level (Huang *et al.*, 2004, Huang *et al.*, 2007a, Huang *et al.*, 2007c, Chan *et al.*, 2004, Xie *et al.*, 2005a, Xie *et al.*, 2005b). SCRS from different strains within the same species are generally highly close to each other, but can still be distinguished through multivariate analysis (principal component analysis, discriminant functional analysis, etc.). Researchers have successfully separated different strains of *E. coli* (Jarvis *et al.*, 2004) and *Acinetobacter sp.* (Maquelin *et al.*, 2006) using this technique

Another essential part of single cell techniques is linking microbial species with their specific functional attributes, because which species contribute to, and how particular microorganisms work within, an ecosystem

is equally, or even more important, than their identification. However, traditional approaches can usually only give limited information about this or have several drawbacks. For example, the traditional SIP method combined with genomic sequencing is irreversibly destructive to microbial communities, thus losing the information about distribution and localization of certain microbes within environmental samples. Raman microspectroscopy however, doesn't require any pre-treatment due to its inherent features, solving this problem in a very user friendly way. In recent years, Huang and co-workers discovered that several carbon-associated bands will shift to a lower wavenumber (red-shift) if ^{13}C -labeled substrates are used as the carbon source (Huang *et al.*, 2004, Huang *et al.*, 2007b, Huang *et al.*, 2009a). Furthermore, there is a liner relationship between the differing percentage of labeled ^{13}C in single cells and the corresponding red shift ratio (Huang *et al.*, 2007b), allowing us to obtain approximate information about how much percent the cells are labeled. This gave scientists the idea about combining Raman microspectroscopy with SIP to perfectly link microorganisms to their ecological functions and even trace the flow of labeled elements (Li *et al.*, 2013) within ecosystems; this works not only for ^{13}C but also ^{15}N -labeled substrate used as a nitrogen source (Huang *et al.*, 2010). Figure 2-2 shows the SCRS (average) difference between ^{12}C and fully ^{13}C -labeled *E. coli* samples. As can be seen, the red-shift occurs in several carbon-associated bands. Amongst them, the band at 1002 cm^{-1} (phenylalanine) in the SCRS of ^{12}C *E. coli* is quite strong and sharp, and it shows the most significant shift from 1002 cm^{-1} (in ^{12}C *E. coli* spectrum) to 965 cm^{-1} (in ^{13}C *E. coli* spectrum).

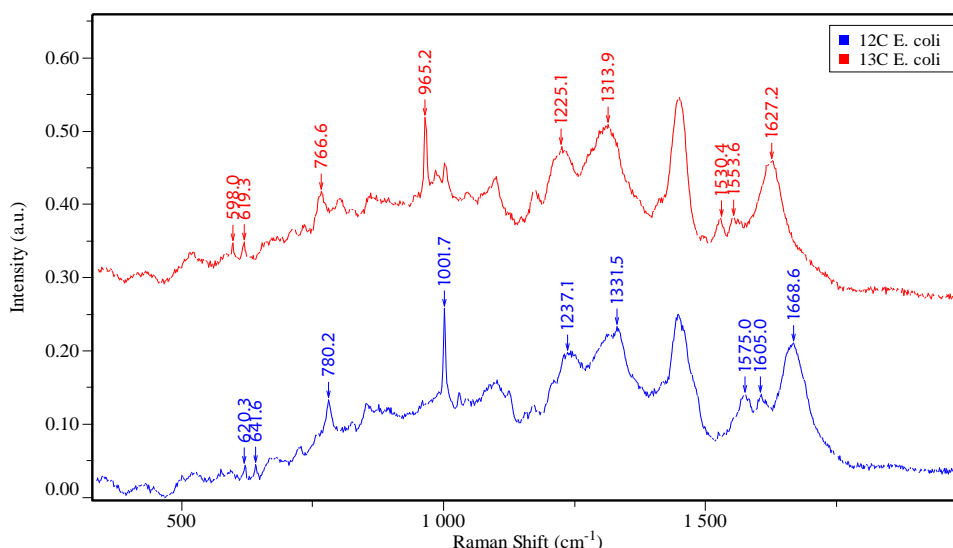


Figure 2-2. The red-shift SCRS comparison between ^{12}C and fully ^{13}C -labeled *E. coli* samples using 532 nm laser (laser power: 35 mW, acquisition time: 20 s). Each SCRS is the average result from 20 replicates.

Additionally, when combining Raman microspectroscopy with FISH, the new Raman-FISH tool (Huang *et al.*, 2007b) will maintain the major advantages from both FISH-MAR and Raman technology, providing a useful method to identify as well as count the labeled cells and study the structure and distribution at a single-cell level within complex microbial communities *in situ*. Raman microspectroscopy is usually coupled with SIP, which enhances this method by allowing the functional profile to be obtained at the same time, making it much more powerful when studying environmental samples. Huang and co-workers have used this tool to successfully identify an unculturable species as playing the most important role in naphthalene biodegradation (Huang *et al.*, 2009a), thus showing the world that the contribution of unculturable microbes cannot be ignored.

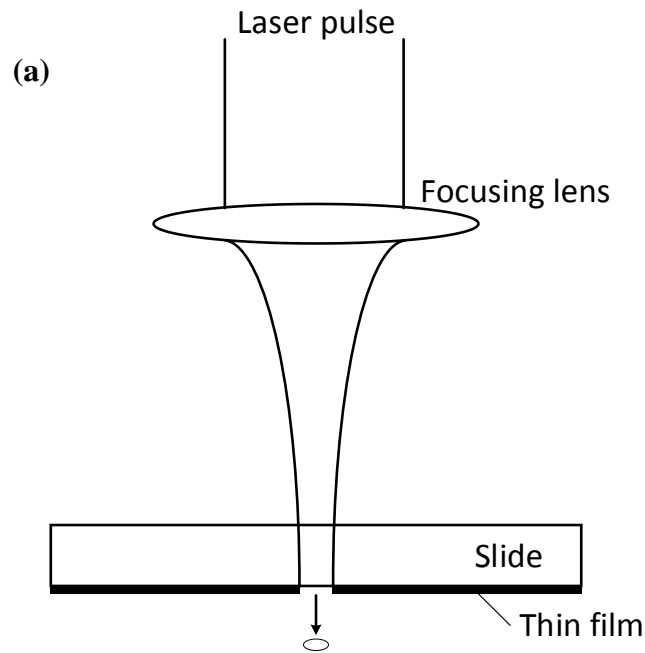
2.4.3 Isolation of single cells

Single cell isolation is the most important section of single cell study, for acquiring DNA is an essential part of microbiological research and the key to opening up the world of the “unseen majority” of bacteria (Whitman *et al.*, 1998). More importantly, some species may be successfully cultured in

the laboratory if the single cell can survive after isolation, because the term “unculturable microorganism” is not an absolute concept. The isolation of single cells from complex microbial communities in a noninvasive way could have considerable benefits in enabling the culturing of more, as yet unexplored, strains from the environment.

The Raman-tweezers method (Xie and Li, 2002, Xie and Li, 2003, Xie *et al.*, 2005a), which couples Raman microspectroscopy with optical tweezers, can not only measure but also trap any interesting single cells using a laser beam. Traditional single cell Raman measurement techniques cannot measure living cells suspended in aqueous medium like water, because the cells will move away within the acquisition time because of cell motility or Brownian motion (Xie and Li, 2003). Raman-tweezers solves this problem by first capturing the cell so that it stays in the trap during the measurement. This combined technology enables a noninvasive measurement of cells that are still in their natural environment, making it more applicable to environmental samples. Based on this feature, Huang and co-workers established a system to isolate single cells using Raman-tweezers and successfully sorted single yeast cells and ^{13}C -labeled SBW25::Km-RFP cells, some of which were then successfully cultivated (Huang *et al.*, 2009b). This attempt confirmed the possibility of isolating single cells using Raman-tweezers, which were still viable for cultivation. However, this method is not perfect, the main drawback being the long acquisition time (usually 30-120s) (Huang *et al.*, 2010) required to screen and move one trapped cell. This long acquisition time is majorly caused by optical tweezers method, the trapped cell should be moved slowly and carefully to avoid escaping. Therefore, the optimization of time is limited. In order to achieve the goal of rapid screening and sorting without losing any of the advantages of Raman microspectroscopy, Huang and co-workers established the Raman activated cell ejection (RACE) method (Wang *et al.*, 2013) this year, which is a very fast and powerful tool to isolate single cells of interest according to their Raman spectra.

The operating principle of Raman activated cell ejection (RACE) is inspired by another technique called laser-induced forward transfer (LIFT) (Fogarassy *et al.*, 1989, Schultze and Wagner, 1991, Wang *et al.*, 2013). In the RACE technique, the laser beam is changed to pulse mode to provide a strong and instant source of heat. A transparent (usually glass) slide is loaded onto the stage, with a thin light-absorbing film on the bottom side, which holds the dried sample on the surface. A pulsed laser comes from the top and is focused upon passing through the focusing lens. This focused laser pulse instantly heats and melts the target area upon touching the film, allowing the single cell on the film to drop and be collected. For a schematic picture of RACE, as well as a comparison of the screen picture before and after cell ejection, see Figure 2-3.



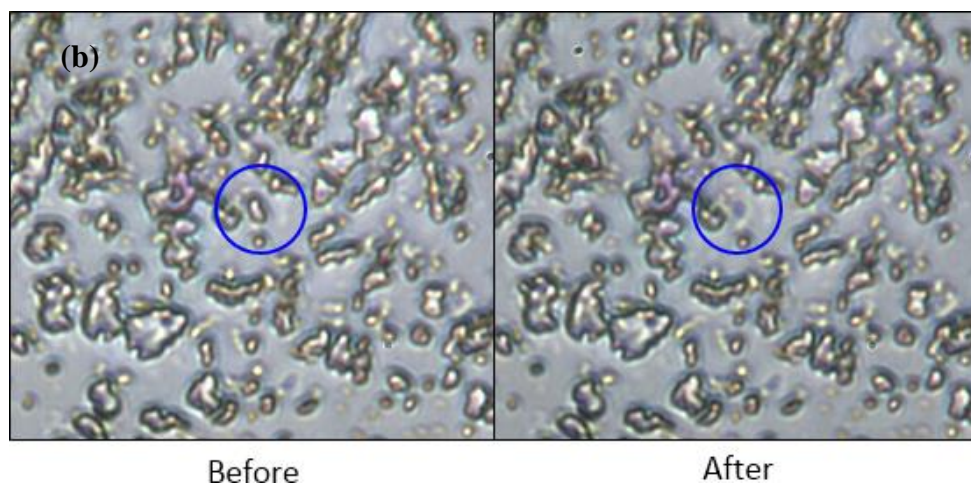


Figure 2-3. (a) Schematic picture of the Raman activated cell ejection (RACE) technique. (b) Comparison of before and after the isolation of a single cell by RACE (50x zoom lens).

Using this principle, the whole cell selection process is extremely quick and can be done at a nanosecond level (time within one pulse). In addition, Raman microspectroscopy allows the laser beam to be focused on a tiny area, so that isolation of a single cell will not affect the surrounding cells. The essential factors in RACE are the slide material and thickness of the film. The material should be both light-absorbing and provide zero background in the range of 500-3000 cm^{-1} in SCRS in order to accurately identify the interested cell before ejection. Furthermore, the film thickness should be neither too thick nor thin, as this will lead to a failure to get an intact cell. The slide used in this project was purchased from Wellsens Ltd., Beijing, China, which has previously proved workable in measuring and isolating single cells by RACE.

Instead of directly ejecting a single cell, another approach to isolate the interested cell, based on the same principle, involves slightly moving the slide and cutting the membrane surrounding the cell using the pulsed laser beam, so that the cell will drop together with a small piece of membrane. Unlike cell ejection, this technique enables the isolation of any size and number of cells at once. This similar method, known as laser micro-dissection (Murray, 2007), has been widely used in medical research to cut tissues and had been used to great success in genetic studies, but as yet no researcher has reported the

application of this technology to the single-cell level. The RACE method is still in the initial stages of development and the most important part of this project is to carry out further tests and improvements.

2.5 Summary

All of the methods introduced above are leading techniques in the field of unculturable microorganism research, but are not perfect to comprehensively explore the world of unculturable microbes. Compared with other techniques, single cell Raman microspectroscopy has excellent features to satisfy most demands required in single-cell research, especially when it is combined with other approaches like SIP. Single cell Raman microspectroscopy is an emerging technique, with much potential still to be discovered and many challenges to overcome, but there is no doubt that its prospects will be unlimited. The comparison between different techniques is shown in Table 2-1.

Table 2-1. Comparison of different culture-independent techniques.

Culture-independent technique	Advantage	Disadvantage
Metagenomics	Extract whole genes from mixed samples; discover new functional genes.	Slow and costly when treating large amounts of complex samples; sometimes requires previous knowledge; linkage of species to their functions is limited.
Stable isotope probing	Can link species to functions; able to do genomic analysis; applicable to combination with other techniques.	Irreversibly destructive to cells; cannot reproduce conditions <i>in situ</i> ; cannot show information at the single-cell level.
Fluorescence activated cell sorting	Enables fast and objective cell sorting at the single-cell level; able to acquire cell information.	Requires previous knowledge; does not suit anything other than aqueous media; invasive to cells; fluorescence is not quantitative.
Single cell Raman microspectroscopy	Label-free and noninvasive; no pre-treatment; fast and easy to identify and differentiate cells at the single-cell level; can link species to functions; enables isolation of individual living cells; compatible with many other techniques.	Long acquisition time in Raman-tweezers technique; not yet mature enough to allow rapid screening and isolation.

Chapter 3: **Materials and methods**

Chemicals and Growth Media

Generally, cells were incubated in Luria-Bertani (LB) medium (Fisher Scientific, UK) at 37 °C, overnight unless otherwise stated.

Pseudomonas putida UWC1 (GFP) cells used in section 4.4 were incubated in LB-agar medium overnight at 37 °C. The LB-agar medium contains Luria-Bertani (LB) broth (Fisher Scientific, UK), noble agar (Sigma, UK) and kanamycin sulphate (Invitrogen, Canada); 20g of LB broth and 15g noble agar were used when making the medium, the final concentration of kanamycin was 50 µg/mL.

The minimal medium (MM) (see Appendix 2 for the recipe) was used to incubate the new *Micrococcus* strain (see section 4.1). Cells were incubated in LB, MM and MM without NH₄Cl overnight at 30 °C.

The M9 minimal medium (for the recipe, see Appendix 3) with fully D-labeled glucose (10mM) was used to incubate different D-content *E. coli* samples (see section 4.2.2) overnight at 37°C.

The M22 medium (see Appendix 4 for the recipe) was used to incubate carotenoids-containing *Rhodobacter* cells (see section 4.1) overnight at 30 °C.

PR-containing samples used in section 4.1, and SIP samples used in section 4.2 were kindly provided by other researchers (see Acknowledgements).

For the information about strains used in this study and their description, as well as growth conditions, see Table 3-1.

Table 3-1. List of strains used in this study and their growth conditions.

Strain	Description	Growth conditions	Note	
<i>Rhodobacter</i>	Carotenoids containing	M22 medium, overnight, 30 °C	See section 4.1	
<i>Ralstonia eutropha</i> H16	Chemotrophic bacterium, able to use H ₂ as energy source and CO ₂ as carbon source.	LB medium overnight, 30 °C	See section 4.1	
<i>Escherichia coli</i>	Alkane production	LB medium, overnight, 37 °C, 150 rpm	See section 4.1	
	Control			
	PR-expressing. Plasmid: pBAD proteorhodopsin; induced; retinal added.	LB medium, overnight, 37 °C, 150 rpm		See section 4.1; Provided by Prof. Neil Hunter and Michaël Cartron from University of Sheffield.
	PR control. Plasmid: pBAD proteorhodopsin; induced; noretinal.			
	PR control. Plasmid: pBAD proteorhodopsin; uninduced; retinal added.			
	PR control. Plasmid: pBAD proteorhodopsin; uninduced; no retinal.			
	PR control. Plasmid: pBAD empty; uninduced; retinal added.			
	PR control. Plasmid: pBAD empty; uninduced; no retinal.			
	PR control. Plasmid: pBAD empty; induced; retinal added.			
PR control. Plasmid: none; uninduced; no retinal not contained.				

	PR control. Plasmid: none; uninduced; retinal added.		
	PR-expressing minicells	LB medium, overnight, 37 °C, 150 rpm	See section 4.1; Provided by Prof. Neil Hunter and Micha ě Cartron from University of Sheffield.
	0% D-labeled	M9 Minimal medium with 10mM fully D- labeled glucose, overnight, 37 °C, 150 rpm	See section 4.2.2
	5% D-labeled		
	10% D-labeled		
	25% D-labeled		
	50% D-labeled		
	75% D-labeled		
	100% D-labeled		
	E. coli AR3740	LB-agar medium	See section 4.3
	E. coli AR3741		
	E. coli AR3859		
	E. coli ATCC 25922		
<i>Micrococcus</i>	Carotenoids and cytochrome expressed	LB/MM/MM no NH ₄ Cl, overnight, 30 °C, 150 rpm	See section 4.1
<i>Methylophaga marina</i>	0% ¹³ C-labeled		See section 4.2.1; Provided by Prof. Colin Murrell, Oliver Burns and Carolina Grob from University of East Anglia.
	10% ¹³ C-labeled		
	20% ¹³ C-labeled		
	40% ¹³ C-labeled		
	60% ¹³ C-labeled		
	80% ¹³ C-labeled		
	90% ¹³ C-labeled		
	100% ¹³ C-labeled		

<i>Methylomonas methanica</i> MC09	0% ¹³ C-labeled		See section 4.2.1; Provided by Prof. Colin Murrell, Oliver Burns and Carolina Grob from University of East Anglia.
	20% ¹³ C-labeled		
	40% ¹³ C-labeled		
	60% ¹³ C-labeled		
	80% ¹³ C-labeled		
	90% ¹³ C-labeled		
	100% ¹³ C-labeled		
	Environmental microbial communities	MNPs-free	
<i>Pseudomonas putida</i> G7	100% D-labeled		See section 4.2.2; Provided by Dr. Aliyu Ibrahim Dabai from Queen's University Belfast
	0% D-labeled		
	0% D-labeled	<i>Pseudomonas putida</i> F1	See section 4.2.2; Provided by Dr. Aliyu Ibrahim Dabai from Queen's University Belfast
	10% D-labeled	<i>Pseudomonas putida</i> F1	
	25% D-labeled	<i>Pseudomonas putida</i> F1	
	50% D-labeled	<i>Pseudomonas putida</i> F1	
	75% D-labeled	<i>Pseudomonas putida</i> F1	
	100% D-labeled	<i>Pseudomonas putida</i> F1	
<i>Pseudomonas</i> AR5196	LB-agar medium		See section 4.3
<i>Pseudomonas</i> ATCC 10145			

	<i>Pseudomonas</i> ATCC 9027		
	<i>Pseudomonas putida</i> UWC1 (GFP)	LB-agar medium with 50 µg/mL Kanamycin, overnight, 37 °C, 150 rpm	See section 4.4
<i>Citrobacter</i>	<i>Citrobacter</i> AR3030 <i>Citrobacter</i> AR3870 <i>Citrobacter</i> AR3871 <i>Citrobacter</i> AR8090	LB-agar medium	See section 4.3
<i>Enterobacter</i>	<i>Enterobacter</i> ATCC 13048 <i>Enterobacter</i> ATCC 35030 <i>Enterobacter</i> SN122	LB-agar medium	See section 4.3
<i>Enterococcus</i>	<i>Enterococcus</i> AR3906 <i>Enterococcus</i> AR3908 <i>Enterococcus</i> AR4437 <i>Enterococcus</i> ATCC 29212	LB-agar medium	See section 4.3
<i>Klebsiella</i>	<i>Klebsiella</i> AR5236 <i>Klebsiella</i> AR5239 <i>Klebsiella</i> K3875	LB-agar medium	See section 4.3
<i>Staphylococcus aureus</i>	<i>S. aureus</i> AR4182 <i>S. aureus</i> AR4999 <i>S. aureus</i> AR5000 <i>S. aureus</i> ATCC 25923	LB-agar medium	See section 4.3
<i>Streptococcus</i>	<i>Streptococcus</i> B AR3938 <i>Streptococcus</i> B AR4186 <i>Streptococcus</i> B AR4255 <i>Streptococcus</i> B AR4256	LB-agar medium	See section 4.3

Raman Microspectroscopy and RACE

All cell samples were centrifuged (3500 rpm, 10 min) and re-suspended in deionized water three times to get pure individual cells. Slides used in the experiments below were: calcium fluoride (CaF₂) slides; glass slides with special coating (called “ejection slide” in Chapter 4); and glass slides with a special mixed membrane (Wellsens Ltd., Beijing, China). Each cellular suspension (2 μL) was spread on a slide and air-dried before starting Raman analysis. SCRS were harvested using a LabRAM HR 800 confocal Raman microscope (Horiba Scientific, UK). The resolution used in this study is either 1.5 cm⁻¹ using 600VIS grating or 2-3 cm⁻¹ using 300 grating. A 100× magnifying dry objective (NA=0.90, Olympus, UK) was used to focus laser on single bacterial cells and collect Raman signal. A 50× magnifying dry objective (NA=0.55) was used to focus laser pulse on the membrane surface in RACE technique. A 532 nm Nd:YAG laser (Torus, Laser Quantum Ltd., UK) was used for Raman measurement and cell isolation. Labspec 5 software (Horiba Scientific, UK) was used to manipulate Raman system and record Raman spectra. For the measurement of single cell Raman spectra, the constant laser beam was used. The maximum laser power at the sample was 35mW, the laser filter and acquisition time were specified in each study. The percentage of laser filter means the remaining percentage of laser after going through the filter (e.g. 100% filter means full laser power). Multiple single cells were randomly chosen and measured in each sample. For single cell isolation, the 532 nm pulsed laser beam (ALPHALAS GmbH, Germany) was used, pulse energy is 8 μJ and pulsed time is 1 second. In the study in section 4.4, in order to get the correct sequencing result, the “cutting” method was used (see section 2.4.3) to get multiple cells in one sample. Isolated cells were then collected with 1.5 mL sticky microtubes (AdhesiveCap 200 clear, Carl Zeiss Microscopy, Germany).

SCRS Data Analysis

Labspec 5 software (Horiba Scientific, UK) was used to record, normalized, averaged Raman spectra and export their spectra images. Specifically, the procedures of normalization were: first, moves all traces to the minimum intensity level; then, normalizes all the traces to same area value (100).

MATLAB R2013a software (MathWorks, USA) was used to do discriminant functional analysis (DFA) in section 4.3. DFA codes were generated by Dr. Roy Goodacre from the University of Manchester. DFA codes for MATLAB was programmed based on Manly's principles (Manly, 1994).

Single Cell Gene Sequencing

The whole genome of isolated single cells was amplified using the REPLI-g Single Cell Kit (QIAGEN Ltd. UK). Single cell DNA amplification was used strictly following the manufacturer's instruction. Polymerase chain reaction (PCR) was performed, the primers of which were 63f and 1387r in 16S PCR, and GFP_ADPI_for and GFP_ADPI_rev1 for PCR of *Pseudomonas putida* UWC1 (GFP) samples (see Appendix 5 for PCR reaction mixture and program, Appendix 6 for primers). The DNA amplified products and PCR products were examined by running an agarose gel (see Appendix 7). The PCR products were then purified using the QIA quick PCR Purification Kit (QIAGEN Ltd. UK) according to the manufacturer's instruction. After purification, the PCR products were sent for sequencing at the Core Genomic Facility, Medical School, University of Sheffield. Bacterial species were identified using the DNA sequence in the NCBI BLAST search engine.

Raman Single-Cell Detection list

Natural biomarkers (section 4.1):

- Carotenoids in *Rhodobacter*
- Unique Raman band in *Ralstonia eutropha* H16

- Distinction between alkane synthesizing *E. coli* and wild-type *E. coli*
- Proteorhodopsin in *E. coli* at the single-cell level
- Carotenoids and cytochrome in an unknown *Micrococcus* strain

Raman-SIP (section 4.2):

- ¹³C-labeled *Methylophaga marina*
- ¹³C-labeled *Methylomonas methanica* MC09
- ¹³C-labeled MNPs-free environmental sample
- Deuterium Raman band in *Pseudomonas* and *E. coli*

Multivariate data analysis (section 4.3):

- 29 samples multivariate data analysis

Single cell ejection and gene sequencing (section 4.4):

- Single cell ejection of ¹³C-labeled MNPs-free cells
- Single cell isolation and gene sequencing of *Pseudomonas putida* UWC1 (GFP)

Chapter 4: **Results and discussion**

As mentioned in section 1.2, the technique of single cell Raman microspectroscopy is subdivided into 3 steps: (1) identify single cells from microbial communities, by searching for biomarkers in Raman spectra; (2) isolate interesting individual cells after identifying the specific microbial species, through development of the RACE technique; (3) amplify and DNA sequence genes from isolated single-cell samples.

Previous research was primarily concentrated on the observation of biomarkers and came up with several significant achievements. Several typical peaks from particular biochemical compounds in SCRS were discovered and used to identify specific microbial species (see section 4.1). Also, when combined with SIP, the unique variations in SCRS caused by certain stable isotopes helped us to link microbial species with their functions, giving a better understanding of how they take part in the ecosystem (see section 4.2). Meanwhile, multivariate data analysis was applied in SCRS data analysis among different microbial species, proving that the single cell Raman technique can successfully distinguish between various species (see section 4.3). On the subject of single cell isolation and gene sequencing, preliminary studies were carried out giving positive results that indicated the feasibility of the RACE technique (see section 4.4).

4.1 Searching for natural biomarkers in SCRS

Several particular biochemical compounds have been shown to give unique Raman signals in spectra. In some microbes these specific biomarkers have helped researchers understand their biological function or condition, as well as to rapidly detect and distinguish the cells from other strains. Whilst searching for original biomarkers, the single cell Raman technique has successfully revealed specific Raman bands for carotenoids in *Rhodobacter sp.*, and cytosine/uracil in *Ralstonia eutropha* H16 cells. In addition, for the first time, proteorhodopsin could be observed at the single-cell level, and the

advanced applications of this signal are being investigated. Also, an unidentified strain was found, which contained both carotenoids and cytochrome bands in its Raman spectra.

The Raman signal of carotenoids

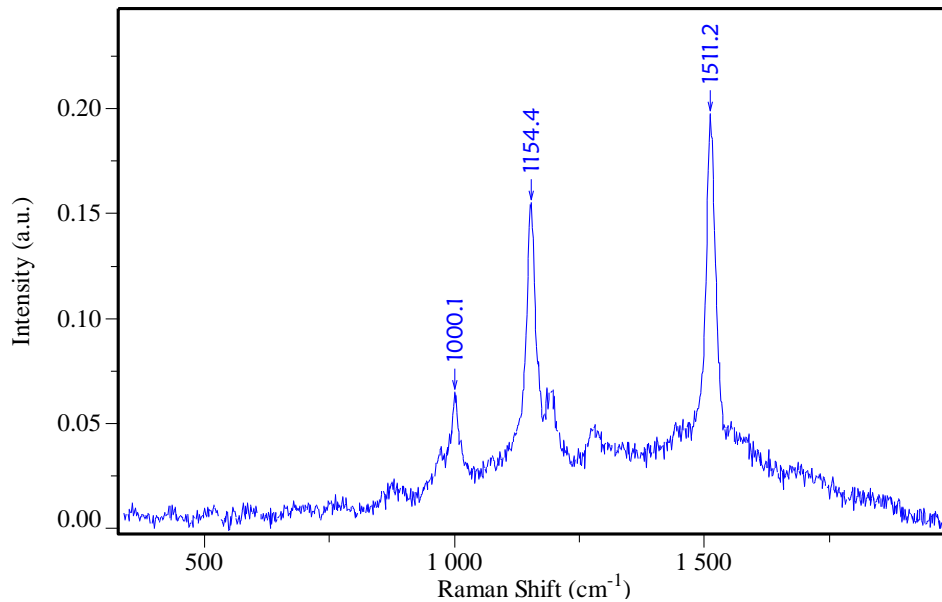


Figure 4-1. The averaged and normalized SCRS from 20 replicates of *Rhodobacter sp.* (acquisition time: 1s).

Figure 4-1 shows the averaged and normalized SCRS from 20 replicates of *Rhodobacter sp.* single cells. Cells were spread on the ejection slide. The laser filter was 1% and the acquisition time was 1s.

As is shown above, there are 3 strong and sharp peaks (1000.1 cm^{-1} , 1154.4 cm^{-1} , 1511.2 cm^{-1}) shown in the SCRS image, which are the typical signals of carotenoids (Li *et al.*, 2012). Carotenoids play an essential role in bacterial photosynthesis and light harvesting. When it comes to the Raman technique, these strong and rapid signals allow them to be useful biomarkers to identify *Rhodobacter sp.* within 1 second, laying the foundation for their possible rapid screening in mixed microbial communities.

Unique band in SCRS of *Ralstonia eutropha* H16

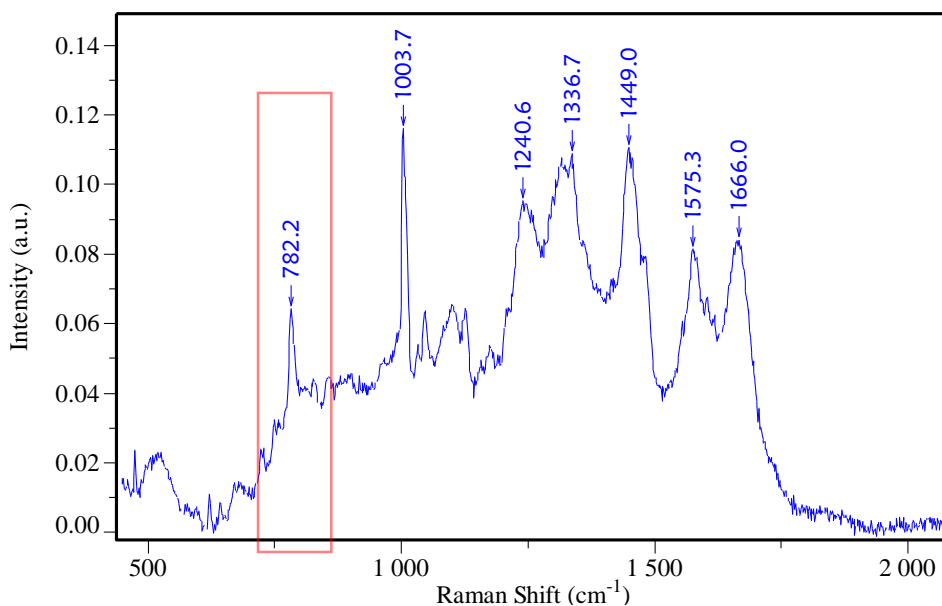


Figure 4-2. The averaged and normalized SERS from 20 replicates of *Ralstonia eutropha* H16 (acquisition time: 30s).

Figure 4-2 shows the averaged and normalized SERS from 20 replicates of chemotrophic *Ralstonia eutropha* H16 single cells. Cells were spread on the CaF₂ slide. The laser filter was 100% and the acquisition time was 30s to harvest clear spectra. Unlike other SERS images, a unique peak, which was relatively strong and sharp, appeared at 782.2 cm⁻¹. This band is representative of cytosine/uracil in cells. However, the Raman band of either cytosine or uracil is normally weak, and why *Ralstonia eutropha* H16 has such high Raman band is unclear. This band can be used as a useful biomarker to instantly recognize this strain from other bacteria.

Change of C-H stretching intensity in SCR of alkane synthesizing *Escherichia coli*

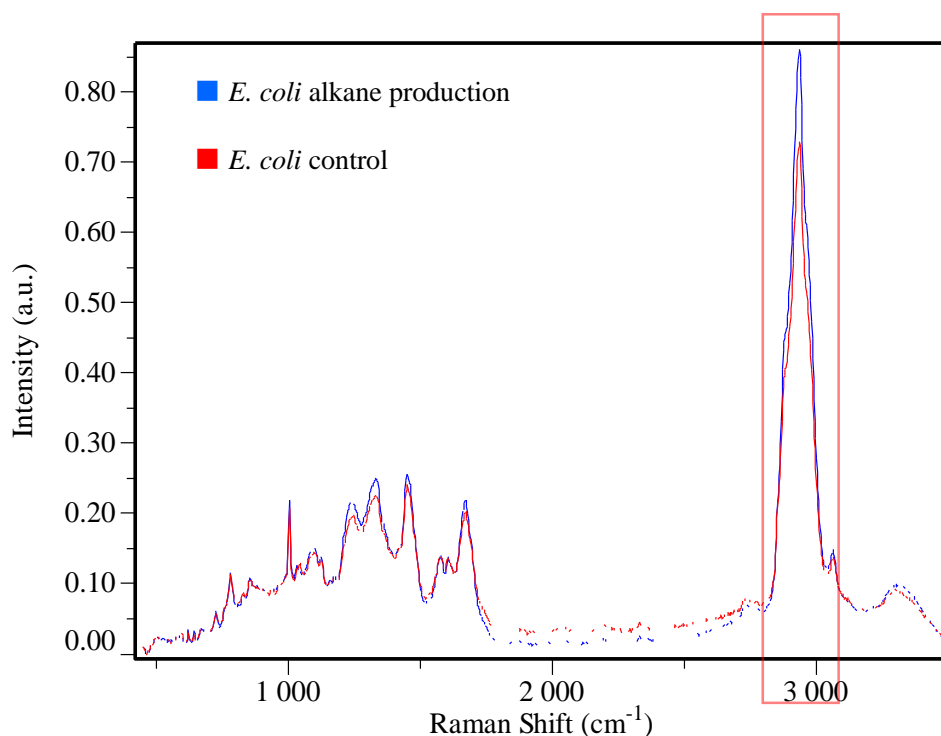


Figure 4-3. The averaged and normalized SCRS from 20 replicates of alkane synthesizing *E. coli* samples and *E. coli* control sample (acquisition time: 20s).

Figure 4-3 shows the difference between averaged and normalized SCRS of 20 replicates of an *E. coli* strain which is engineered for alkane synthesizing and the normal wild-type *E. coli* strain that acts as a control. Cells were spread on the CaF₂ slide. The laser filter was 100% and the acquisition time was 20s, which are the same conditions used when measuring the normal control *E. coli* cells.

An obvious significant difference is discovered in the intensity around 2936.6 cm⁻¹, which is the signal of C–H stretching. The SCRS of the alkane synthesizing *E. coli* strain doesn't reveal any shift in wavenumber, but the peak of C–H stretching is much stronger and sharper when compared to that of the *E. coli* control strain.

To quantitatively calculate the enhancement of C–H stretching Raman intensity in the alkane synthesizing *E. coli* strain SCRS, the ratio of the intensity data between 2936.6 cm⁻¹ (the signal of C–H stretching) and 1003.6

cm^{-1} (the signal of phenylalanine) was used to estimate the change in the intensity of C–H stretching. The intensity of phenylalanine is widely used as a reference in ratio calculation in Raman spectra analysis. There are several reasons for this choice: first, all cells contain phenylalanine, regardless of their microbial species; second, the Raman signal of phenylalanine is very clear; moreover, the intensity of phenylalanine is strong, sharp, and usually stable.

The $2936.6 \text{ cm}^{-1}/1003.6 \text{ cm}^{-1}$ results from alkane producing *E. coli* and *E. coli* control are shown in Figure 4-4, using 20 replicates and using \pm standard error for the error bar.

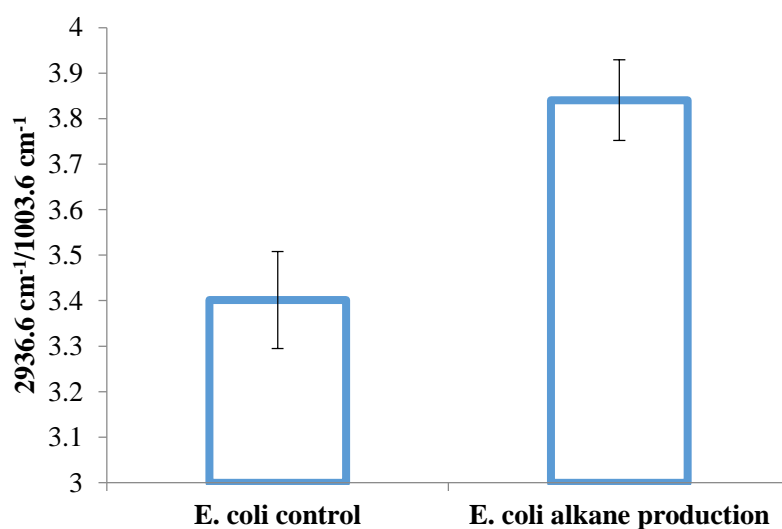


Figure 4-4. Ratio of $2936.6 \text{ cm}^{-1}/1003.6 \text{ cm}^{-1}$ of averaged and normalized SCRS from 20 replicates of alkane synthesizing *E. coli* samples and *E. coli* control sample.

From Figure 4-4, the convincing enhancement of C–H stretching Raman intensity can be observed in alkane synthesizing *E. coli* SCRS compared with the control, their respective error bars indicating the reliability of this increase. As a result, single cell Raman measurement allows researchers to detect alkane synthesizing cells, which provides an opportunity to combine single cell Raman microspectroscopy with synthetic biology in future applications.

Proteorhodopsin (PR) Raman signal in *Escherichia coli*

Proteorhodopsin (PR) is a microbial protein that plays the role of a light-driven proton pump. It was widely discovered in oceanic microbial communities, including proteobacteria, flavobacteria, cyanobacteria and archaea. PR has not been found in culturable microbes, but when cloned and expressed in *E. coli*, PR could correctly combine with its cofactor retinal and work as a light-dependent proton pump (Béjà *et al.*, 2000, Beja *et al.*, 2001). The Raman signal of PR at the single-cell level hasn't been reported so far.

In this study, a total of 9 *E. coli* samples under different conditions were measured by single cell Raman microspectroscopy. The information on each sample is shown in Table 4-1. Theoretically, sample 1 should be the only one that contains functional PR with the other 8 samples serving as various controls.

Table 4-1. Sample information of PR-expressed *E. coli*.

Number	Cell type	Plasmid	Induced	Retinal
1	BL21	pBAD Proteorhodopsin	+	+
2	BL21	pBAD Proteorhodopsin	+	-
3	BL21	pBAD Proteorhodopsin	-	+
4	BL21	pBAD Proteorhodopsin	-	-
5	BL21	pBAD Empty	-	+
6	BL21	pBAD Empty	-	-
7	BL21	pBAD Empty	+	+
8	BL21	None	-	-
9	BL21	None	-	+

All 9 samples were spread on the ejection slide. The laser power was 80% of maximum power, and the laser filter was 1%. The exported laser power had to be weak as PR was easily bleached by laser beams; on the other hand, if the laser power was too weak, a clear spectra could not be harvested. Through the results in pre-experiments, 1% laser filter is proper to get a relatively clear SCRS without destroying the PR signal. The acquisition time

was 120s to obtain clear spectra. Each averaged Raman spectra was the mean of 20 individual cells. The results are shown in Figure 4-5.

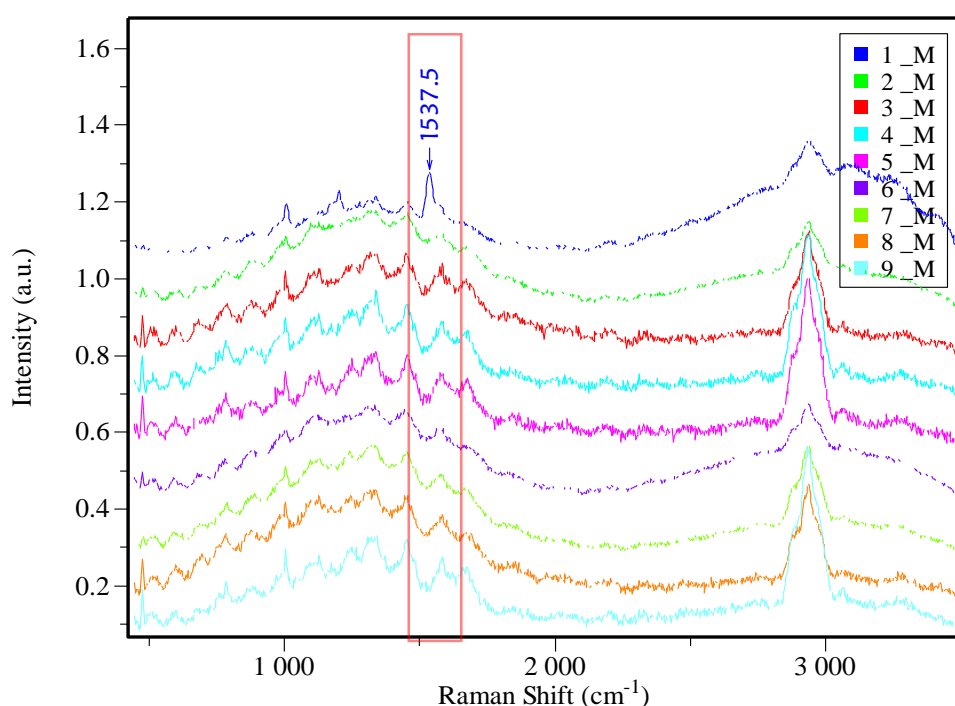


Figure 4-5. The averaged and normalized SCRS from 20 replicates of proteorhodopsin-expressing *E. coli* single cells (acquisition time: 120s).

As is shown in Figure 4-5, PR was successfully expressed around 1536 cm^{-1} in sample 1, whilst the other control samples did not show this particular signal as expected. Although many researchers have discovered PR previously, this is the first time the Raman signal of PR in prokaryotes has been observed at the single-cell level. With this knowledge of the specific PR signal, we are now able to easily identify single cells that contains PR using Raman microspectroscopy.

To reach the goal of rapid screening when faced with large amounts of complex environmental cells, the acquisition time was optimized to 3s to observe the characteristic peak around 1536 cm^{-1} . The image of a single cell Raman spectrum in 3s is shown in Figure 4-6.

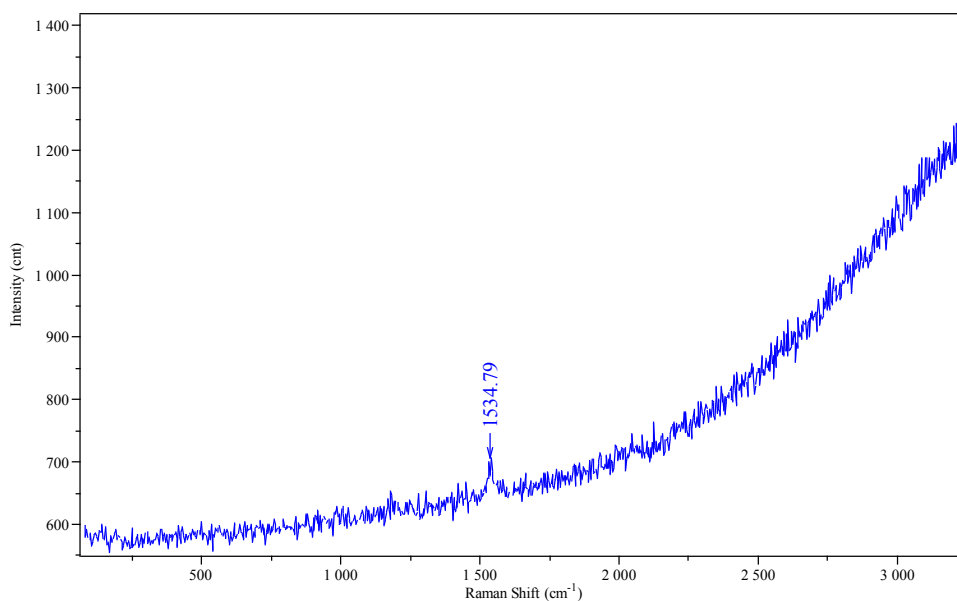


Figure 4-6. The SCRS for rapid screening of a PR-containing *E. coli* single cell (acquisition time: 3s).

It may be noticed that the wavenumber of PR in Figure 4-6 has a 3 cm^{-1} error compared to that in Figure 4-5. This error is quite natural in this experiment, because the resolution used in PR measurement is 300 grating, which would result to a 3 cm^{-1} error. The highest intensity of PR may not be recorded because of this resolution, and the highest intensity that recorded in the spectrum may be the signal on the shoulder. As a result, the wavenumber of PR may be close but different in various SCRS. On the other hand, the variety of individual cells and random error caused in the measurement may contribute to an error as well. In either possibility, the PR signal is not hard to be recognized, for there is no obvious disturbing signal near 1536 cm^{-1} .

As well as normal cells, the SCRS shows that PR was also observed in mini-cells. The main difference between mini-cells and normal cells is that mini-cells are smaller and anucleate, which means that they may contain RNA and proteins but lack a cell nucleus, just like blood cells. Though they don't contain any DNA, PR can still be obviously detected in *E. coli* MC1000 mini-cells under the same measurement parameters. For the picture of an *E. coli* MC1000 mini-cell and a typical spectrum, see Figure 4-7.

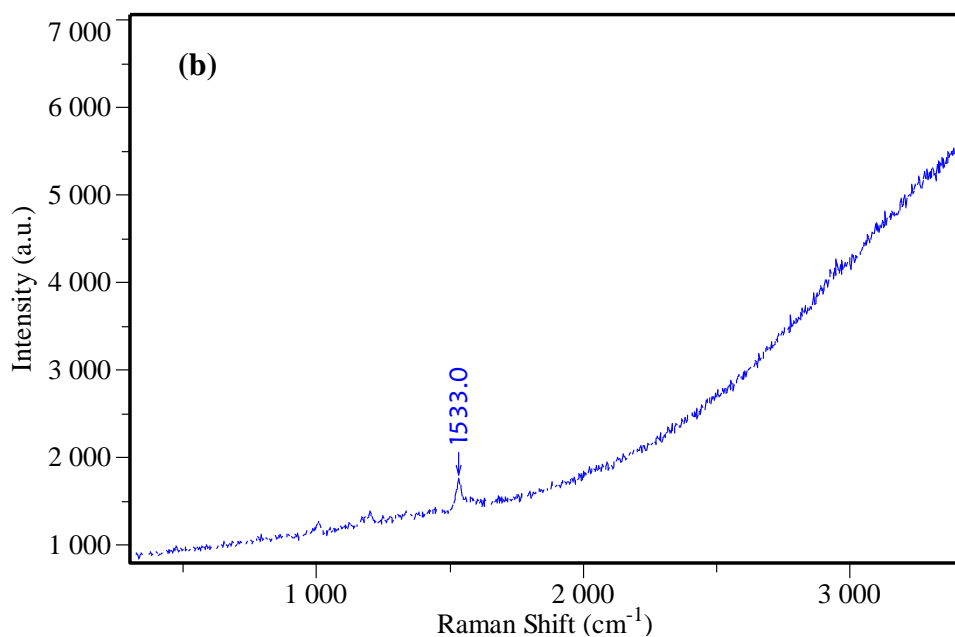


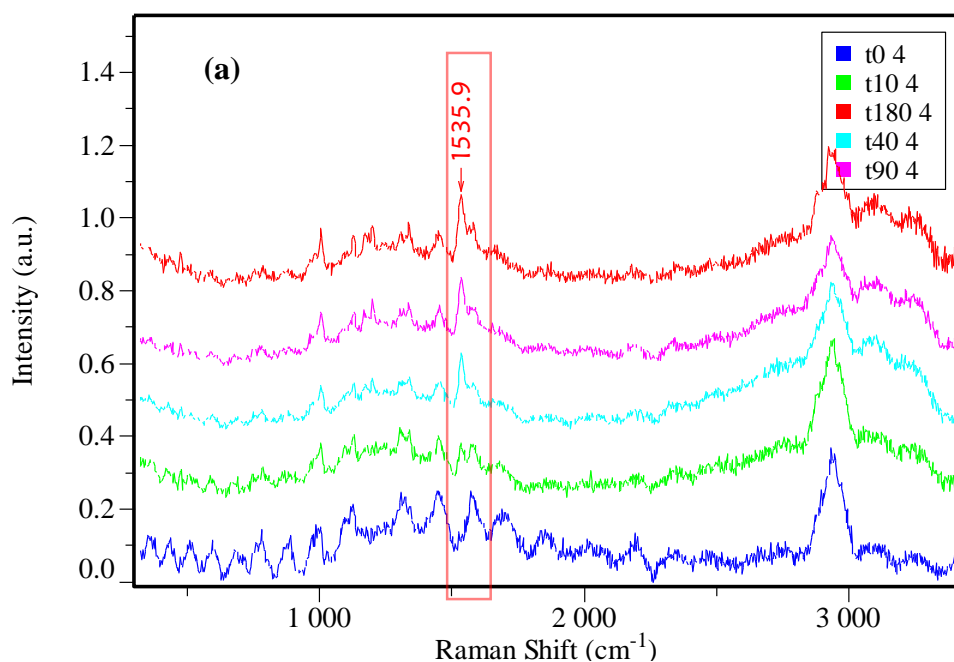
Figure 4-7. (a) The image of an *E. coli* MC1000 mini-cell (100× zoom lens). (b) A typical Raman spectrum of a PR-containing MC1000 mini-cell (acquisition time: 120s).

Since PR can be observed in *E. coli* at the single-cell level, it provides an opportunity to observe the process of PR formation through analysis of the intensities in SCRS. Thus, a further experiment was designed to make a brief dynamic analysis of PR formation in single cells. Four PR-containing *E. coli* samples were analyzed in this experiment under the same measurement parameters, with details of the samples shown in Table 4-2.

Table 4-2. Sample information of PR-expressing *E. coli* cells used in dynamic analysis.

Number	Cell type	Plasmid	Induced	Retinal
1	BL21	pBAD Proteorhodopsin	-	-
2	BL21	pBAD Proteorhodopsin	-	+
3	BL21	pBAD Proteorhodopsin	+	-
4	BL21	pBAD Proteorhodopsin	+	+

All the samples were incubated at 30 °C after L-arabinose induction. The time points for measurement are $t = 0$, $t = 10$ min, $t = 40$ min, $t = 90$ min, and $t = 180$ min. At each time point, 6 individual cells were randomly chosen for measurement in each sample. The SCRS intensity around 1536 cm^{-1} of the PR-expressing sample 4 was seen to increase over time, whilst the other 3 controls remained the same. The time-course of sample 4 induction is shown in Figure 4-8 (a). The comparison between the 4 samples is shown in Figure 4-8 (b), taking $t = 180$ min as an example.



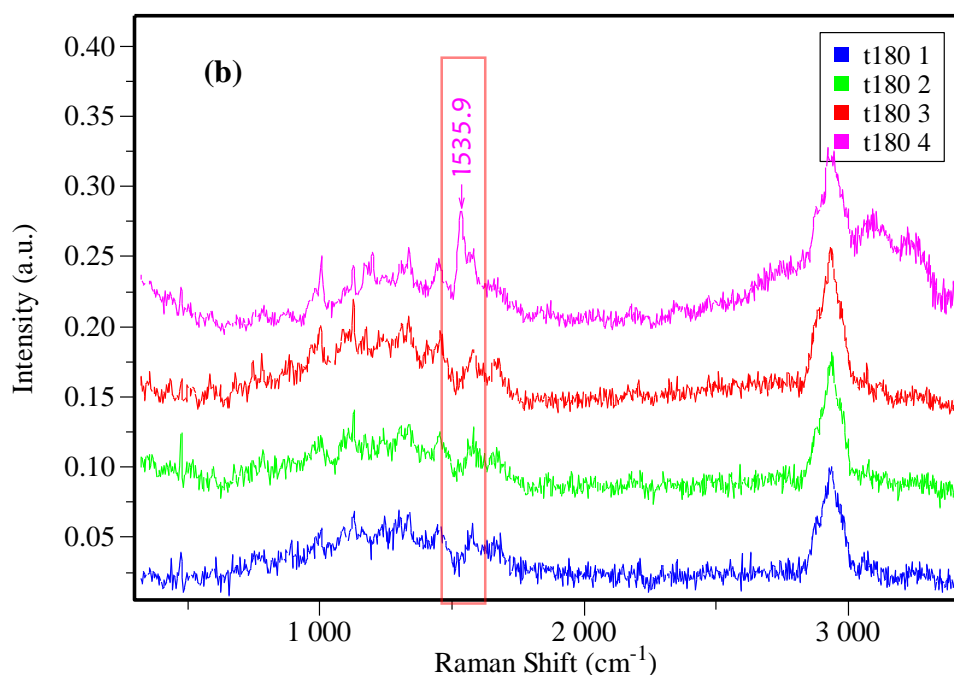


Figure 4-8. (a) PR formation of sample 4 in averaged and normalized SCRS at all the time points (acquisition time: 120s). (b) Comparison around 1536 cm^{-1} in averaged and normalized SCRS between 4 samples at $t = 180$ min (acquisition time: 120s).

To obtain a dynamic analysis of PR formation, intensity ratios of $1536 \text{ cm}^{-1} / 1002 \text{ cm}^{-1}$ in a total of 30 SCRS (6 replicates \times 5 time points) from sample 4 were calculated. The SCRS of controls may not show a clear phenylalanine band, because there is a phenomenon that the cell without PR will harvest a spectrum with weaker intensity compared to that with PR under same measurement conditions. Because the laser power was weak in order to harvest clear PR band, the Raman signals of sample 1, 2 and 3 would not as clear as sample 4. The reason why SCRS of cells that contain PR could observe stronger intensities stays unknown, there is a possibility that PR could enhance the intensity of whole spectra. However, the average spectra of controls could observe a clear phenylalanine band; moreover, the clear phenylalanine can always be observed in SCRS from PR-contained individual cells at $t = 180$ min, and for that reason the intensity of phenylalanine was still be chosen as a reference. At each time point, the averaged result and

standard error was calculated from 6 replicates. The ratio – time dynamic curve of PR is shown in Figure 4-9, taking \pm standard error as the error bar.

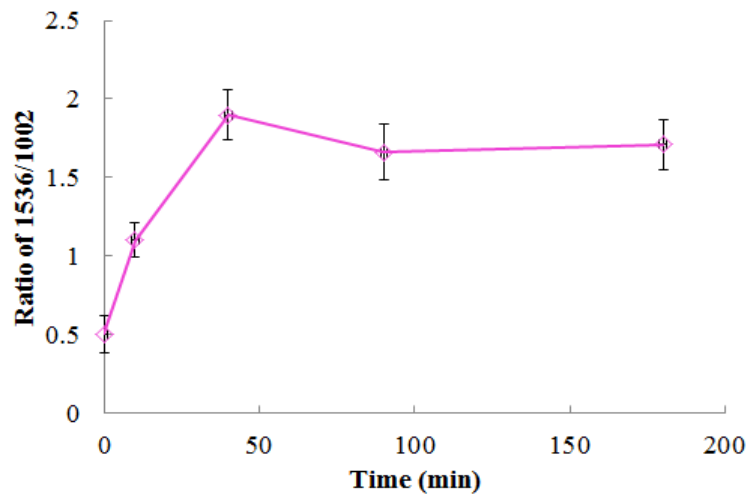


Figure 4-9. Ratio – time dynamic curve of PR, calculated from 6 replicates in sample 4 at all 5 time points.

Due to the lack of time points and replicates, the dynamic curve has some errors especially at the $t=40\text{min}$ point. However, a trend can still be observed showing roughly that PR intensity increases rapidly after induction and is close to saturation within 90 minutes. This dynamic analysis is obviously very brief and more time points as well as replicates are required, but the long acquisition time of measurement (120s) makes it impossible to get spectra from so many cells between two time points, especially in the first 60 minutes after induction. Also, the washing and drying times (see Chapter 3) of each sample required before taking measurements are also long. However, the drying procedure could not be ignored for 2 reasons. One is the limitation from the equipment, that cells in aqueous media could not be seen clearly under the microscope, nor could the lens touch the surface of water. The other is that the target cell would move away due to cell motility or Brownian motion within the acquisition time. The optical tweezers method was once used to test whether PR can be measured in water using Raman-tweezers but didn't obtain any meaningful spectra, probably the critical laser

power was one of the reasons for the failure. Perhaps an alternative method needs to be designed to obtain a more detailed dynamic analysis of PR formation.

In conclusion, what we have already discovered is that proteorhodopsin can be recognized at the single-cell level, and its signal was strong and sensitive enough to be observed within 3s, which means it can be regarded as a reliable biomarker to achieve rapid screening. As mentioned above, PR is widely found in marine microorganisms, where it acts as a light-driven proton pump and is essential for many marine microbial species. Therefore, the results shown here have the potential to be used in a future application for the rapid analysis of complex marine samples.

Carotenoids and cytochrome bands in a new *Micrococcus* strain

A new yellow *Micrococcus* strain that can be grown in minimal medium (MM) (see Appendix 2) overnight was recently found in Dr. Huang's laboratory. Growth in MM is an uncommon phenomenon for *Micrococcus sp.* as *Micrococcus* cells have always been reported as needing organic compounds as a carbon source, although they can easily grow on inorganic nitrogen. Moreover, this strain has a fairly fast growing speed, for it normally takes days for bacteria using inorganic carbon and nitrogen to grow. To find out if there is anything unique in the phenotype of this unknown strain, Raman measurements were taken to get spectra from single cells.

Cells were incubated overnight in 30 °C in 3 different media: LB, MM, and MM without NH₄Cl. After incubation, washed cells were spread on the CaF₂ slide. Figure 4-10 (a) shows the microscope image of *Micrococcus* cells, which were normally organized as tetrads. The laser filter used in measurement is 100% and the acquisition times are 1s for LB-incubated cells and 2s for MM-incubated cells and cells grown in MM no NH₄Cl. Results are shown in Figure 4-10 (b).

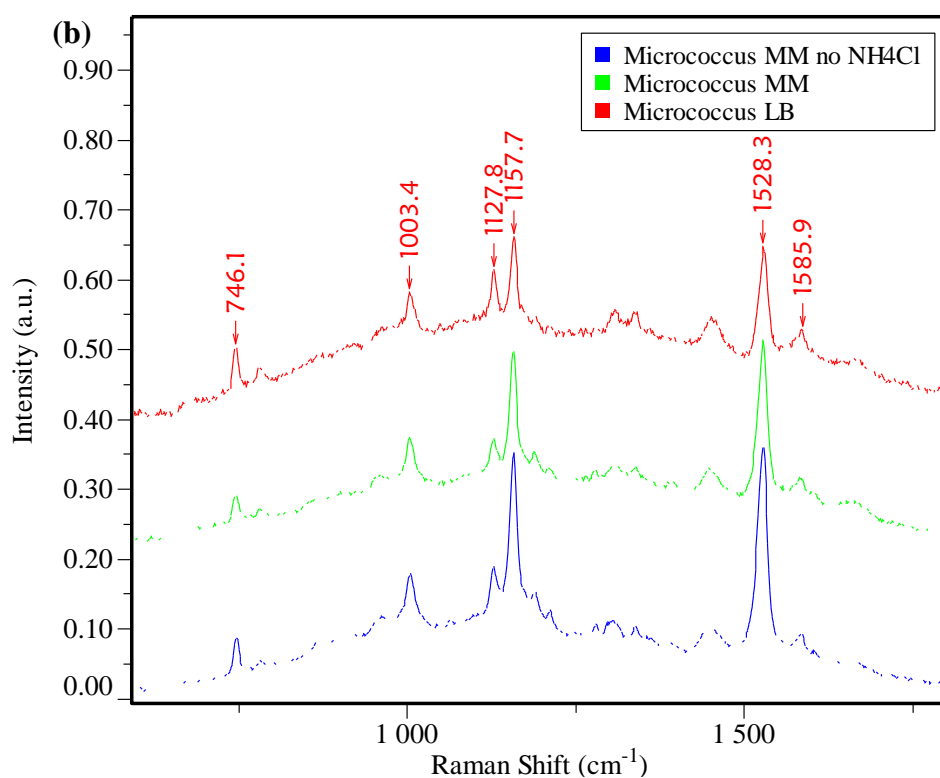
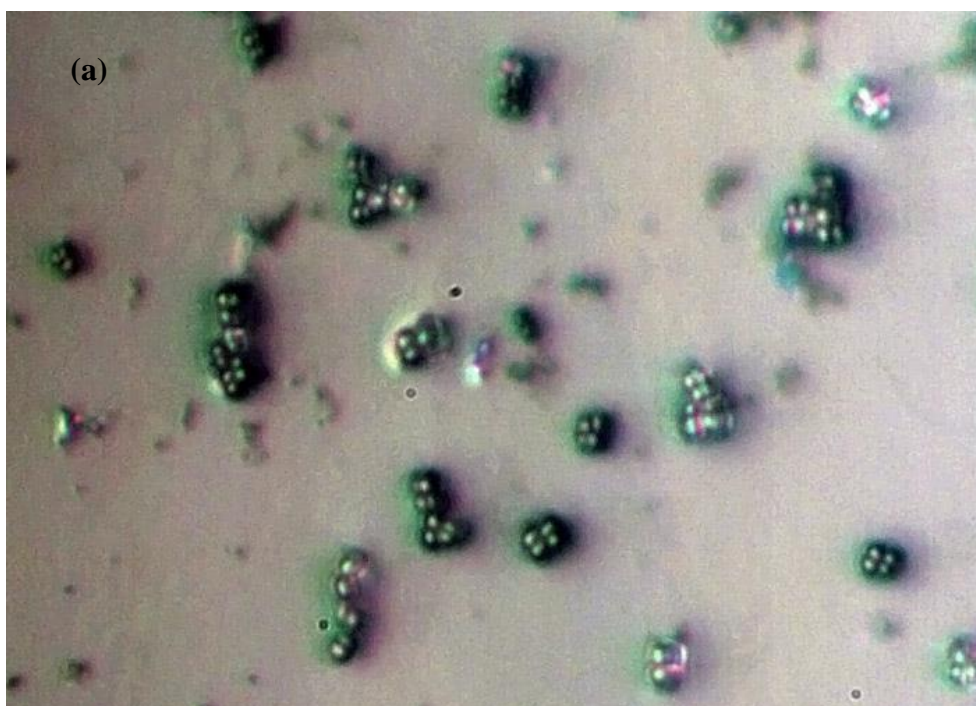


Figure 4-10. (a) Microscope image of the new *Micrococcus* strain (100×zoom lens). (b) The averaged and normalized SCRS from 20 replicates of the *Micrococcus* strains incubated in LB, MM and MM without NH₄Cl.

Several conclusions can be derived from the SCRS results. Firstly, there are 2 biomarkers apparent in the spectra at the same time, one from carotenoids (1003, 1157, 1528 cm^{-1}) (Li *et al.*, 2012) and the other from cytochrome c (746, 1127, 1586 cm^{-1}) (Okada *et al.*, 2012). Cytochrome is common in *Micrococcus* bacteria, but as yet no researcher has ever found a *Micrococcus* strain containing carotenoids at the same time, which indicates the uniqueness of this new bacterium. Secondly, all 3 samples grew in their respective media and their spectra were just the same, which means this strain can absorb nitrogen from air for growth if lacking a nitrogen source, and carotenoids will be created whether or not a carbon source is provided. All these results indicated the uniqueness and great potential of this new strain. For any future studies, these 2 biomarkers will definitely be strong enough to allow for rapid identification, screening, and maybe some functional analysis.

4.2 Raman-SIP measurement

SIP-associated Raman microspectroscopy is one of the most promising approaches to link microbial species to their functions in environmental communities. In this project, most samples, including *Methylophaga marina*, *Methylomonas methanica* MC09 and a mixed environmental eco-water sample were labeled with ^{13}C and significant Raman shifts were successfully observed. Furthermore, a totally new stable isotope, deuterium (D), was also tested in *Pseudomonas putida* cells and proved to be workable.

4.2.1 Measurement of ^{13}C -labeled cells

Using the measurement of ^{12}C and fully labeled ^{13}C *E. coli* single cells as a standard database (see Figure 2-2), *Methylophaga marina* and *Methylomonas methanica* MC09 cells were labeled by growth in media containing different percentages of ^{13}C and measured by Raman microspectroscopy in order to obtain a relationship between the Raman shift and percentage of ^{13}C .

SCRS analysis of ^{13}C -labeled *Methylophaga marina*

Methylophaga marina samples were fed with methanol containing various percentages of ^{13}C . The information on all 8 samples is shown in Table 4-3.

Table 4-3. Sample information for ^{13}C -labeled *Methylophaga marina*.

sample	^{12}C Methanol		^{13}C Methanol	
	Percentage (%)	Amount (μL)	Percentage (%)	Amount (μL)
1	100	250	0	0
2	90	225	10	25
3	80	200	20	50
4	60	150	40	100
5	40	100	60	150
6	20	50	80	200
7	10	25	90	225
8	0	0	100	250

Cells were spread on the ejection slide. The laser filter was 25% and the acquisition time was 15s. The result of averaged and normalized SCRS from 20 replicates in each sample can be seen in Figure 4-11. As is revealed in the figure, there is Raman-shift from 780, 1001, and 1671 cm^{-1} in 100% ^{12}C -SCRS to 766, 965, 1622 cm^{-1} in 100% ^{13}C -SCRS.

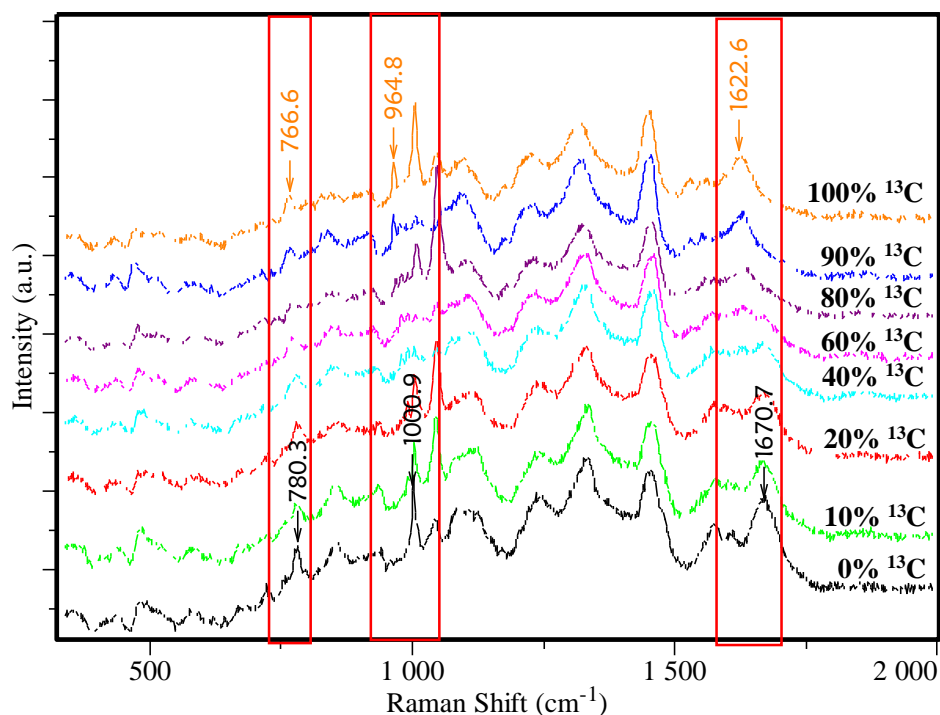


Figure 4-11. The averaged and normalized SCRS from 20 replicates of different ^{13}C -content labeled *Methylophaga marina* (acquisition time: 15s).

Generally, the shift from 1001 cm^{-1} to 965 cm^{-1} should be the most significant marker, but this band was suspected to have been disturbed by the unknown peak at 1043 cm^{-1} in ^{12}C -SCRS in this case. In order to have a better ratio – ^{13}C percentage curve, the protein band from 1671 cm^{-1} in 100% ^{12}C -SCRS to 1622 cm^{-1} in 100% ^{13}C -SCRS was chosen to do analysis. Intensity ratios of $1622\text{ cm}^{-1}/1671\text{ cm}^{-1}$ in a total of 160 SCRS (20 replicates \times 8 samples) were calculated. The calibrated ratio – ^{13}C content curve is shown in Figure 4-12, using \pm standard error as the error bar.

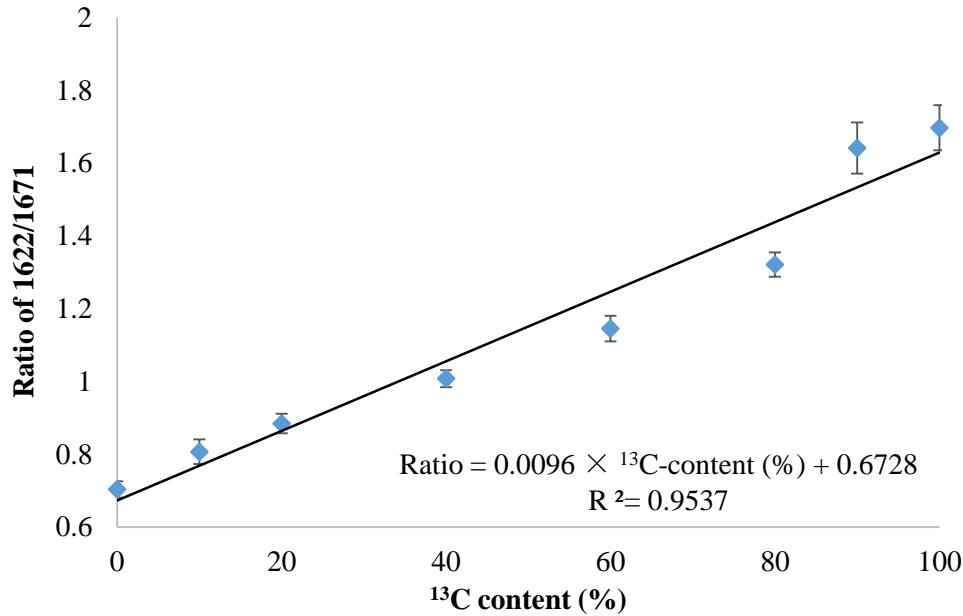


Figure 4-12. Calibration curve of 1622 cm⁻¹/1671 cm⁻¹ ratio - ¹³C content from *Methylophaga marina* SCRS. Calculated from 20 replicates in each sample.

This curve shows a linear relationship between the Raman shift and the ¹³C content. Using this calibration curve, information about the ¹³C content of a single cell can be acquired through SCRS analysis without the need for any other treatment.

SCRS analysis of ¹³C-labeled *Methylomonas methanica* MC09

The percentage of ¹³C in the 8 samples of *Methylomonas methanica* MC09 were just the same as with *Methylophaga marina* samples, except that they were fed with different amounts of methane. The information on all 8 samples is shown in Table 4-4.

Unlike the *Methylophaga marina* samples, signals for carotenoids were found in SCRS. The laser filter was 10% using the ejection slide and the acquisition time was 0.1s to obtain the signals for carotenoids. From the results in Figure 4-13, the Raman shift of all 3 peaks can be observed, from 1007, 1156, 1510 cm⁻¹ in 100% ¹²C-SCRS to 988, 1122, 1477 cm⁻¹ in 100% ¹³C-SCRS.

Table 4-4. Sample information for ^{13}C -labeled *Methylomonas methanica* MC09.

sample	^{12}C Methane		^{13}C Methane	
	Percentage (%)	Amount (mls)	Percentage (%)	Amount (mls)
1	100	6	0	0
2	90	5.4	10	0.6
3	80	4.8	20	1.2
4	60	3.6	40	2.4
5	40	2.4	60	3.6
6	20	1.2	80	4.8
7	10	0.6	90	5.4
8	0	0	100	6

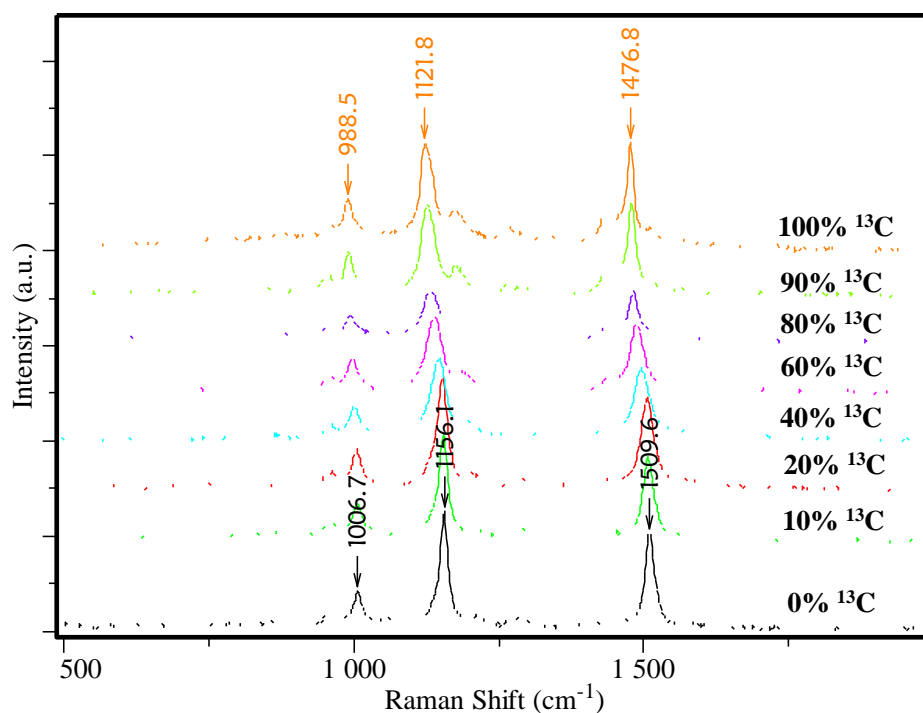


Figure 4-13. The averaged and normalized SCRS from 20 replicates of different ^{13}C -content labeled *Methylomonas methanica* MC09 (acquisition time: 0.1s).

For each carotenoid signal, a wavenumber - ^{13}C content calibration curve of *Methylomonas methanica* MC09 can be created, calculated from 20 replicates each. The results are shown in Figure 4-14, using \pm standard deviation as the error bar.

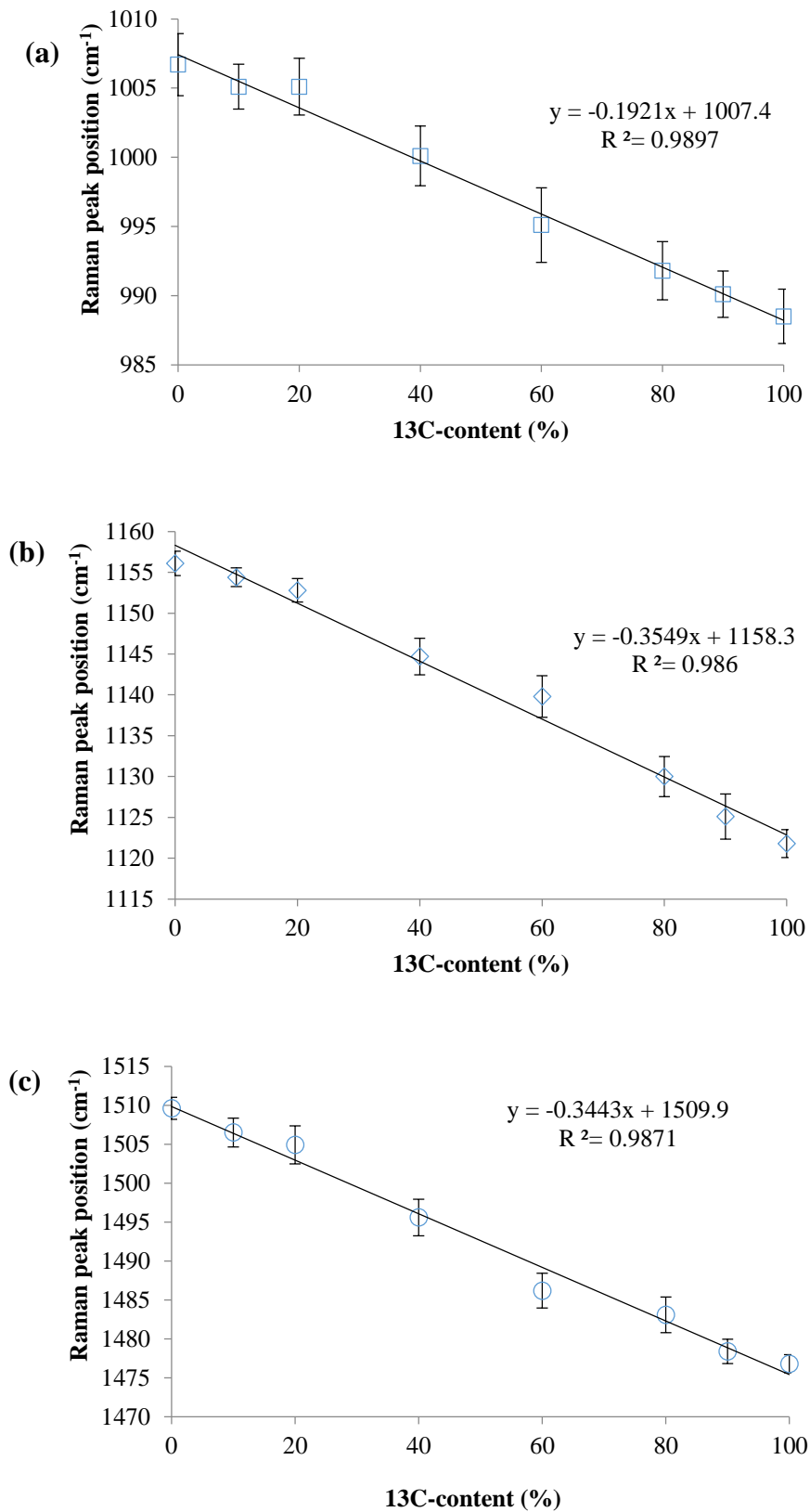


Figure 4-14. (a-c) Calibration curve of Raman peak wavenumber - ¹³C content from *Methylomonas methanica* MC09 SCRS. Calculated from 20 replicates in each sample.

From what is shown in the figure, the Raman shift of the carotenoids revealed an even higher linear regression, although the acquisition time was as short as 0.1s. Because of the cell heterogeneity, different SCRS of single cell may not harvest exactly the same wavenumbers of these 3 peaks, which would cause errors; on the other hand, the resolution of Raman system may also contribute to measurement errors. However, the liner relationship between ^{13}C -content and these 3 Raman peak positions is still obvious. Such a result indicates that carotenoids can be used as a quantitative biomarker for rapid screening as well as for accurately testing the ^{13}C content, which will undoubtedly be of promise in practical applications.

Measurement of ^{13}C -labeled MNPs-free cells from environmental communities

The sample used in this measurement was taken from real environmental communities (Tata Steel wastewater at Scunthorpe, UK) that take part in phenol degradation in eco-water. These complex communities were pre-treated with magnetic nanoparticles (MNPs) and fed with ^{13}C -labeled phenol. To test if the major phenol degrader cells were successfully labeled, the washed communities were spread on the ejection slide, then randomly measured using 25% laser filter and 20s acquisition time. As a result, a Raman shift can be clearly observed in some single cells at 963.5 cm^{-1} , which is the signal of ^{13}C -labeled phenylalanine, while SCRS of some other cells show no apparent shift. Figure 4-15 shows 6 Raman spectra from individual cells, including 3 unlabeled cells and 3 ^{13}C -labeled cells.

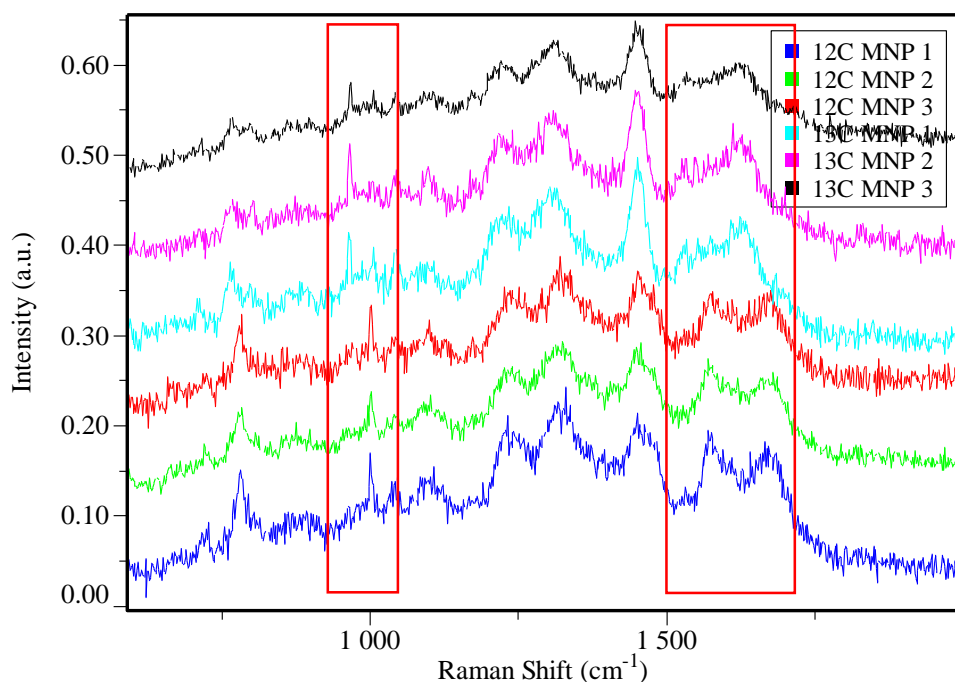


Figure 4-15. The normalized SERS of unlabeled and ^{13}C -labeled MNPs-free single cells (acquisition time: 20s).

The results from the MNPs-free cells confirmed that the Raman-SIP technique can be used on complex environmental communities. Single-cell Raman measurement has successfully identified ^{13}C -labeled cells among mixed microbial communities, which is of great significance to single-cell Raman applications, considering that most previous experiments were measuring pure, cultured samples. Also, the MNPs technique provides an approach to roughly sort stable isotope labeled cells, and in this case, the percentage of labeled cells was about 1/3 of the total, making it easier to find labeled cells in a mixture. With the ability to recognize and localize the major phenol degrader, the identity of the species can be analysed using single cell genomics after isolation using the RACE technique. In fact, ^{13}C -labeled MNPs-free cells were successfully isolated using RACE based on their Raman spectra, but single-cell gene sequencing could not be performed successfully due to contamination (see section 4.4 for detailed discussion).

4.2.2 Measurement of Deuterium-labeled cells

By far, the most wide-used stable isotopes in SIP are ^{13}C and ^{15}N , but few articles have ever studied the effect of deuterium (D, ^2H) labelling. To test if D-labeled cells have any unique bands in SCRS, pure *Pseudomonas putida* G7 cells were fed with 100% D-labeled naphthalene (all hydrogen elements were replaced with deuterium), incubated for 2 days, then spread on the CaF_2 slide to obtain SCRS. Another group of *Pseudomonas putida* G7 cells were fed with unlabeled naphthalene under the same conditions as the negative control. The laser filter used in this measurement was 100% and the acquisition time was 20s, 20 cells were randomly chosen in each sample. The averaged and normalized SCRS results can be seen in Figure 4-16.

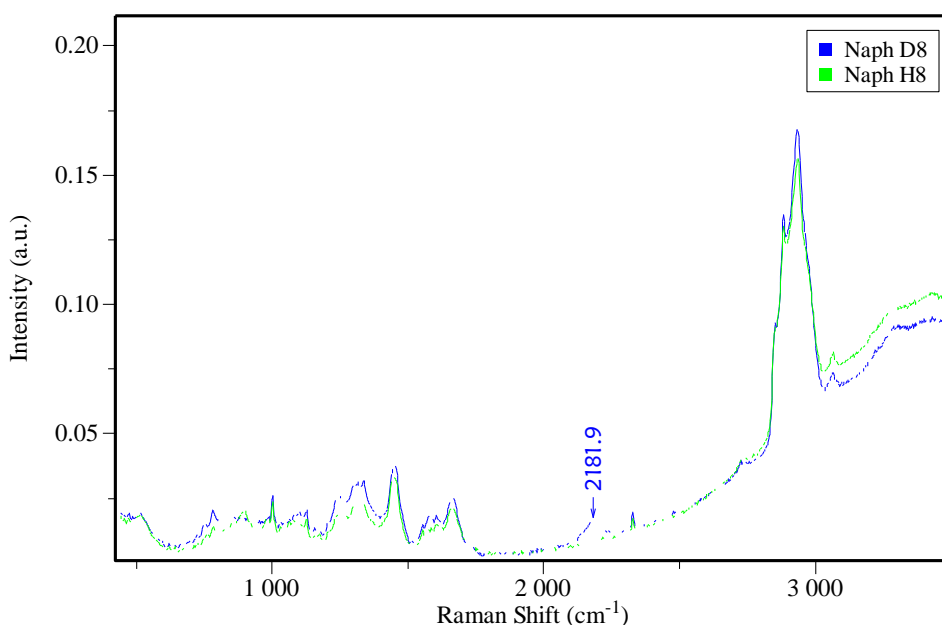


Figure 4-16. The averaged and normalized SCRS from 20 replicates of 100% D-labeled and unlabeled *Pseudomonas putida* G7 single cells (acquisition time: 20s).

Compared with SCRS of unlabeled cells, a relatively flat band occurs at around 2182 cm^{-1} in SCRS of 100% D-labeled cells, which turns out to be the signal of C-D (carbon-deuterium) stretching. This signal was calculated by co-authors and proved to be the Raman shift of C-H stretching, which is the extremely strong band between 2900 cm^{-1} and 3000 cm^{-1} .

This result is meaningful because this is the first time the Raman band of deuterium-labeled compounds has been observed in cells. More importantly, the range from 1900 cm^{-1} to 2500 cm^{-1} in SCRS is the “silent area” that doesn’t contain any natural biochemical profile, so that the signal of C-D can be easily detected and won’t be mixed with other bands. These results indicate that it is practical to label cells with deuterium for Raman analysis.

The “silent area” around the deuterium band makes this band easy to find, and thus provides the possibility of rapid screening by observing the band around 2182 cm^{-1} . By spreading on the ejection slide, the acquisition time can be shortened to 4s using 50% laser filter to catch the band. Figure 4-17 shows a typical Raman spectrum of one cell using 4s acquisition time.

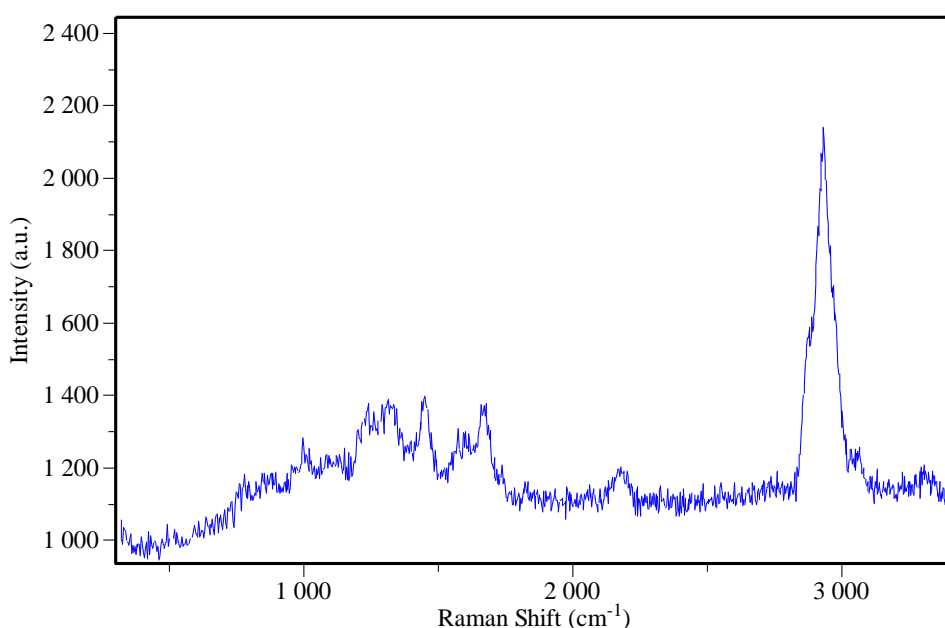


Figure 4-17. The Raman spectrum for rapid screening of a 100% D-labeled *Pseudomonas putida* G7 single cell (acquisition time: 4s).

In order to further study the relationship between different percentages of labeled deuterium and their Raman signals, *Pseudomonas putida* F1 were labeled with different percentage of deuterium (0, 10%, 25%, 50%, 75%, and 100%). For each percentage, 3 biological replicates were prepared, and 10

individual cells were randomly chosen in each biological replicate. Figure 4-18 shows the averaged and normalized SCRS comparison between different percentages of deuterium around 2182 cm^{-1} . It can be seen that the Raman signal from partly D-labeled cells did not show a shift in wavenumber, but changed its intensity in relation to the percentage of deuterium.

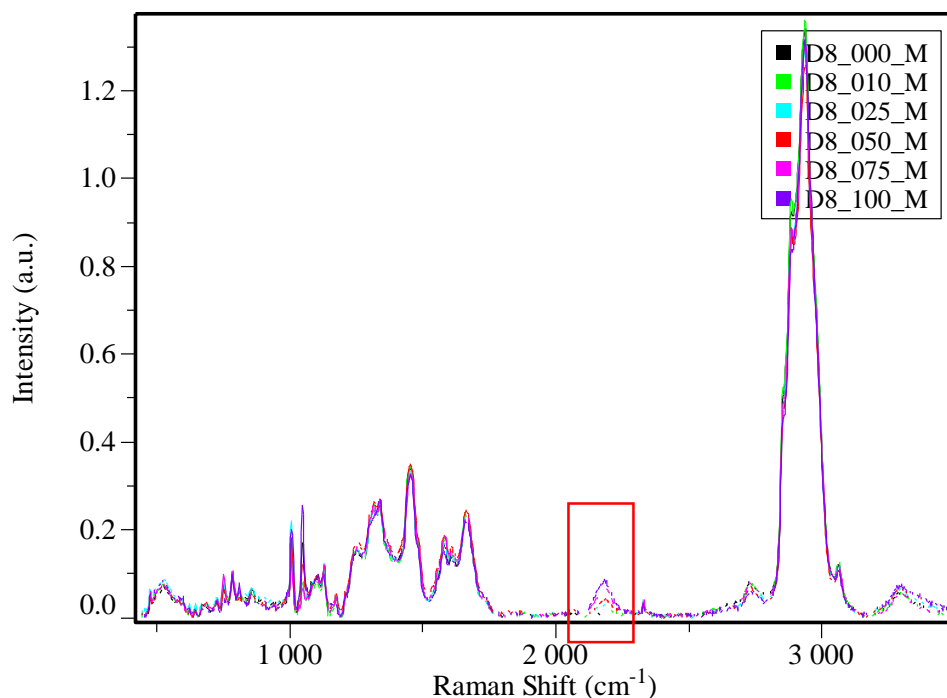


Figure 4-18. The averaged and normalized SCRS from 30 replicates (10 individual cells \times 3 biological replicates) of different D-content labeled *Pseudomonas putida* F1 (acquisition time: 20s).

To find out the relationship between the percentage of deuterium and the intensity of its Raman signal, the ratio of 2182 cm^{-1} /baseline for a total of 180 SCRS (6 percentages \times 10 individual cells \times 3 biological replicates) were calculated. Baseline was determined by averaging the intensities from 1900 cm^{-1} to 2000 cm^{-1} in each spectrum. The final calibration curve is shown in Figure 4-19, using \pm standard error as the error bar.

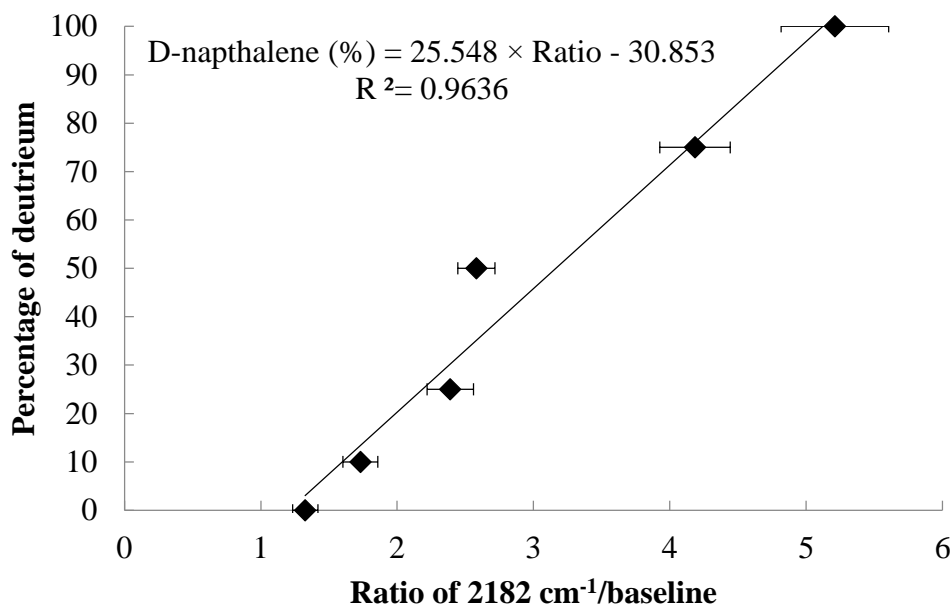


Figure 4-19. Calibration curve of D-percentage – 2182 cm⁻¹/baseline ratio from *Pseudomonas putida* F1 SCRS. Calculated from 30 replicates (10 individual cells × 3 biological replicates) in each sample.

The calibration curve shows a relatively high linear regression between D-percentage and Raman ratio. Thus, for each single cell, the D-content can be roughly calculated from its Raman spectrum.

Since labeled deuterium can be detected through its Raman signal, it is necessary to measure the signal from *E. coli* samples of different D-contents, as *E. coli* is the most widely-used bacterium in microbiology research. To do this, a total of 7 samples were incubated and labeled with various percentages of deuterium (0, 5%, 10%, 25%, 50%, 75%, and 100%). All 7 samples were incubated with M9 minimal medium containing varying amounts of fully D-labeled glucose overnight at 37 °C. After incubation, washed cells were spread on the CaF₂ slide, then measured by Raman with 100% laser filter and 20s acquisition time. With each sample, 30 cells (10 individual cells × 3 biological replicates) were randomly chosen. The SCRS of different D-percentage labeled *E. coli* samples are shown in Figure 4-20.

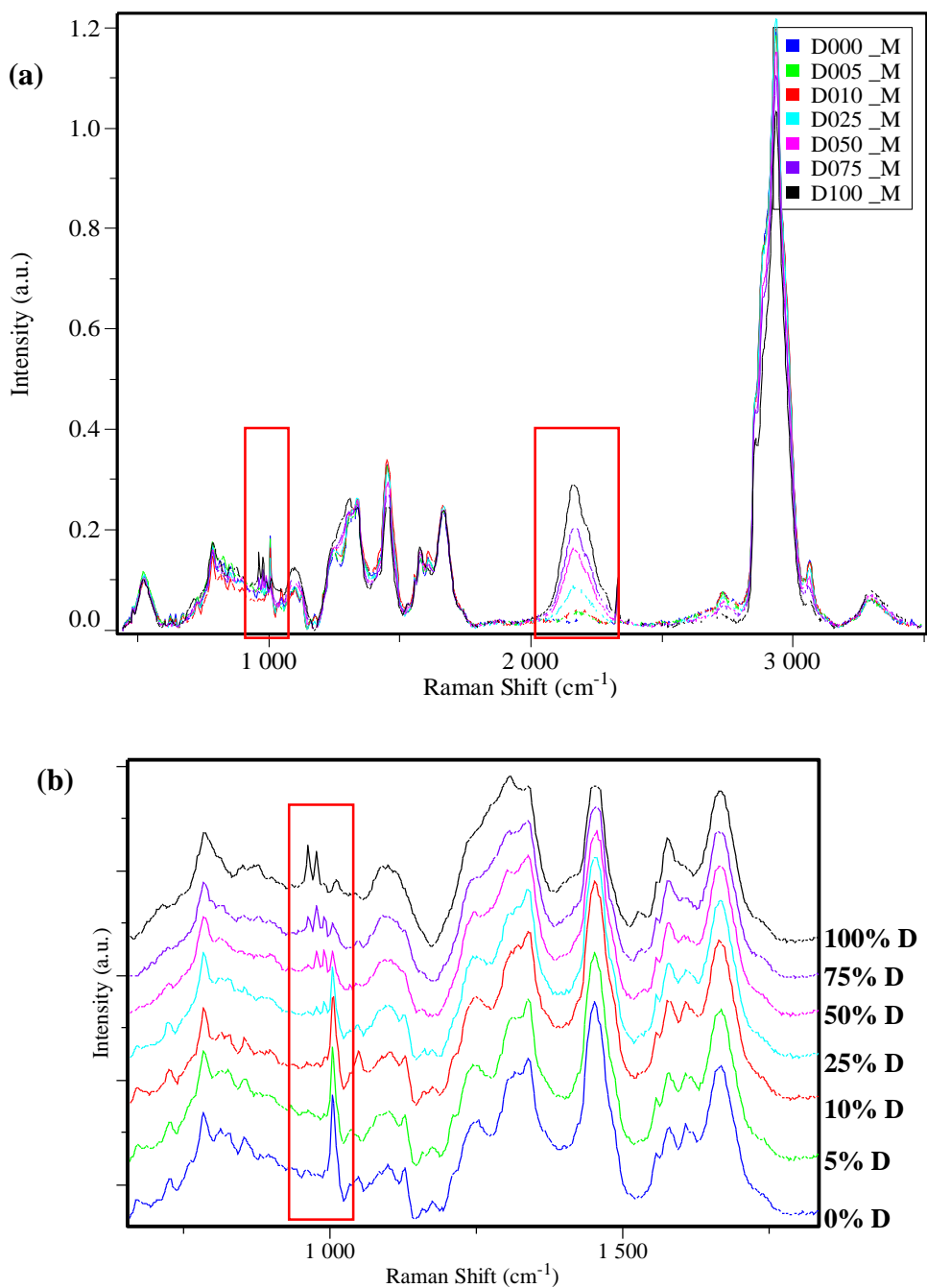


Figure 4-20. (a) The averaged and normalized SCRS from 30 replicates (10 individual cells \times 3 biological replicates) of different D-content labeled *Escherichia coli* cells (acquisition time: 20s). (b) The close view of phenylalanine peak in Figure 4-20 (a).

From the SCRS shown in Figure 4-20 (a), it can be concluded that the signal of deuterium in *E. coli* follows the same rule as with that in *Pseudomonas putida* F1 cells. The intensity of the C-D signal grows as the

deuterium percentage increases. Moreover, the C-D signal in *E. coli* is much stronger and can be observed even at a low deuterium percentage (5%), which is fairly sensitive. Furthermore, it should be noted that the Raman shift of the phenylalanine band occurs in SCRS of D-labeled *E. coli* (see Figure 4-20 (b)), but cannot be observed in *Pseudomonas* cells. This phenomenon suggests that the hydrogen atoms of glucose are used to make phenylalanine in *E. coli* when glucose is present as the sole carbon source; however, *Pseudomonas* cells will not make use of the hydrogen atoms from naphthalene to make phenylalanine.

From the results shown above, deuterium-labeled cells can successfully be detected through SCRS by the change of intensity around 2182 cm^{-1} . The most inspiring thing is that the intensity revealed a linear relationship with the percentage of labeled deuterium, which means that the D-content can be quantitatively measured using Raman microspectroscopy at the single-cell level. Additionally, the deuterium-labeling treatment enables us to achieve the goal of rapid screening, which would dramatically increase the speed when dealing with a large number of complex microbial communities, as long as the D-content is high enough to be detected clearly. The main advantage of D-labeling comparing to ^{13}C -labeling or ^{15}N -labeling is that the price of D-containing substrates is relatively cheap, which would make it more suitable for wide use in functional studies. More importantly, the rapid screening of D-labeled cells is not limited to specific microbial species, because it is determined by the deuterium element itself instead of particular biochemical compounds in cells. This deuterium probing study is very promising and is especially suitable to Raman analysis; it would be a great breakthrough if it could be successfully applied to environmental samples in future experiments.

4.3 Multivariate data analysis of SCRS

In order to test whether this technique is sensitive enough to distinguish between various species and different strains within the same species, a total of 29 pure bacteria samples incubated on LB agar plates were measured, including 8 different bacterial species (see Table 4-5).

Table 4-5. 29 bacterial strains and their IDs in single cell Raman microspectroscopy measurement.

Species	Strain ID	Species ID
<i>Citrobacter</i> AR3030	c1	c
<i>Citrobacter</i> AR3870	c2	c
<i>Citrobacter</i> AR3871	c3	c
<i>Citrobacter</i> AR8090	c4	c
<i>E. coli</i> AR3740	e1	e
<i>E. coli</i> AR3741	e2	e
<i>E. coli</i> AR3859	e3	e
<i>E. coli</i> ATCC 25922	e4	e
<i>Enterobacter</i> ATCC 13048	b1	b
<i>Enterobacter</i> ATCC 35030	b2	b
<i>Enterobacter</i> SN122	b3	b
<i>Enterococcus</i> AR3906	n1	n
<i>Enterococcus</i> AR3908	n2	n
<i>Enterococcus</i> AR4437	n3	n
<i>Enterococcus</i> ATCC 29212	n4	n
<i>Klebsiella</i> AR5236	k1	k
<i>Klebsiella</i> AR5239	k2	k
<i>Klebsiella</i> K3875	k3	k
<i>Pseudomonas</i> AR5196	p1	p
<i>Pseudomonas</i> ATCC 10145	p2	p
<i>Pseudomonas</i> ATCC 9027	p3	p
<i>S. aureus</i> AR4182	s1	s
<i>S. aureus</i> AR4999	s2	s
<i>S. aureus</i> AR5000	s3	s
<i>S. aureus</i> ATCC 25923	s4	s
<i>Streptococcus B</i> AR3938	t1	t
<i>Streptococcus B</i> AR4186	t2	t
<i>Streptococcus B</i> AR4255	t3	t
<i>Streptococcus B</i> AR4256	t4	t

Cells were spread on an ejection slide and 9 individual cells were randomly chosen for measurement in each sample. The laser filter in this study was 25% and the acquisition time was 20 seconds on each cell. The

averaged Raman spectra between different species are shown in Figure 4-21 (a). The spectra between different strains within one species are similar to each other. The spectra of 4 *Citrobacter* strains are shown in Figure 4-21 (b) as an example.

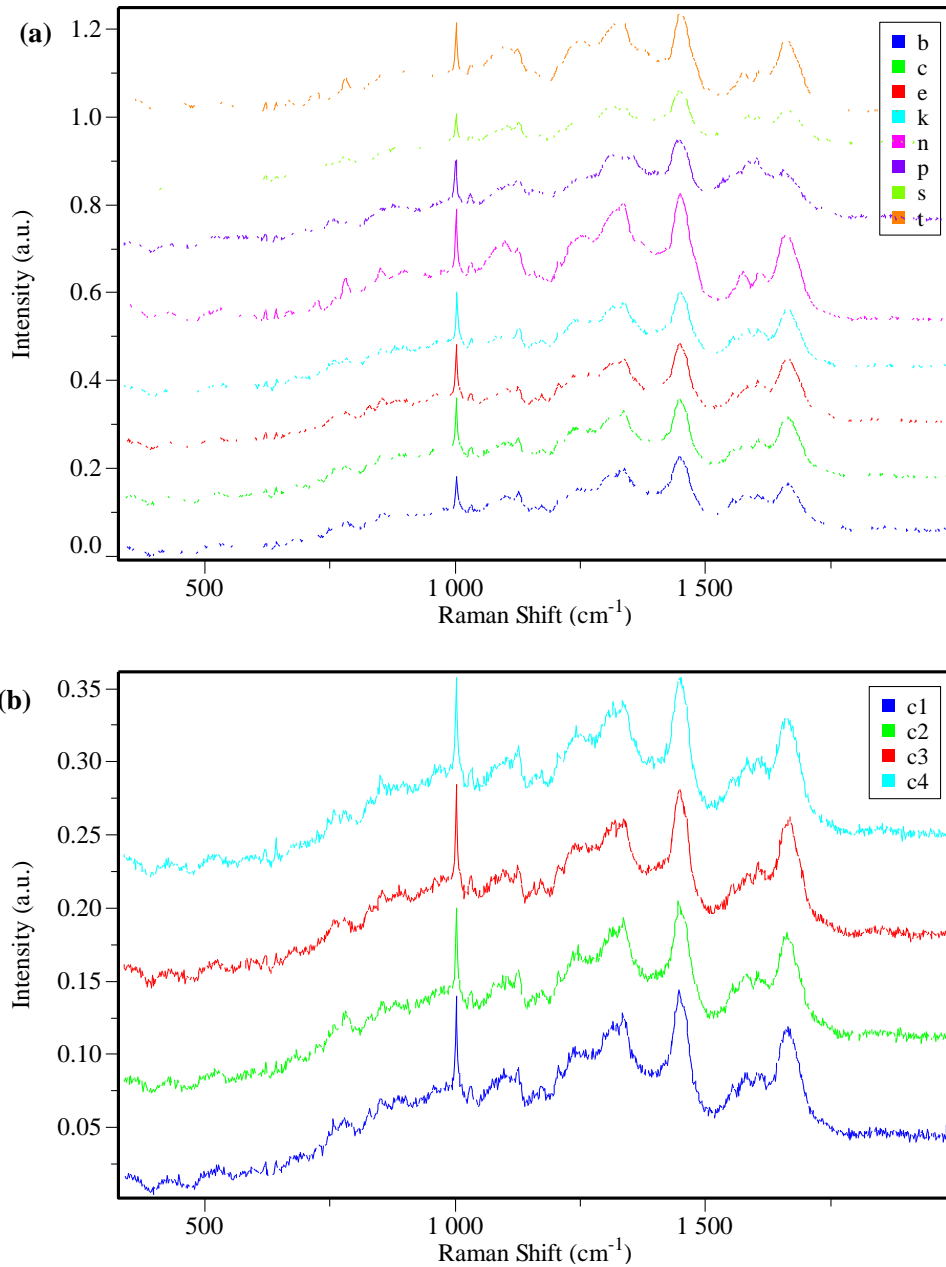


Figure 4-21. (a) The averaged and normalized Raman spectra from 9 replicates of 8 species (*Citrobacter*, *E. coli*, *Enterobacter*, *Enterococcus*, *Klebsiella*, *Pseudomonas*, *S. aureus*, *Streptococcus*). (b) The averaged and normalized Raman spectra from 9 replicates of 4 *Citrobacter* strains.

All 261 Raman spectra (29 strains × 9 replicates) were analyzed using discriminant functional analysis (DFA) to differentiate strains. DFA is a wide-used multivariate analysis to classify data into groups, classes or categories of the same type. It functions by creating discriminant function using predictor variables as independent variables, grouping variables as dependent variables, and differentiate data with these functions. DFA is used when classes are known *a priori*, which is different from principal component analysis (PCA). In this analysis, PCA was primarily used, but failed to successfully classify these species. Therefore, DFA was used to distinguish various microbial species through SCRS data.

The results are shown in Figure 4-22. From the result in Figure 4-22 (a), the n (*Enterococcus*), p (*Pseudomonas*), s (*S. aureus*), and t (*Streptococcus*) can be clearly distinguished from other species, while b (*Enterobacter*), c (*Citrobacter*), e (*E. coli*), and k (*Klebsiella*) were quite mixed with each other, which means they may have similar phenotypes. In order to have a better classification, another DFA analysis was made for the mixed 4 species (see Figure 4-22 (b)). This time the mixed different species were successfully separated, although they were still close to each and a few individual spectra may be mixed with those of other species. These results prove the ability to separate different species using SCRS, which is useful when analyzing complex environmental samples. The data from different strains within one species were neither totally mixed nor separated and this may be because of phenotypic similarities and cellular heterogeneity. More replicates may be required if there is a requirement to separate various strains from within the same species.

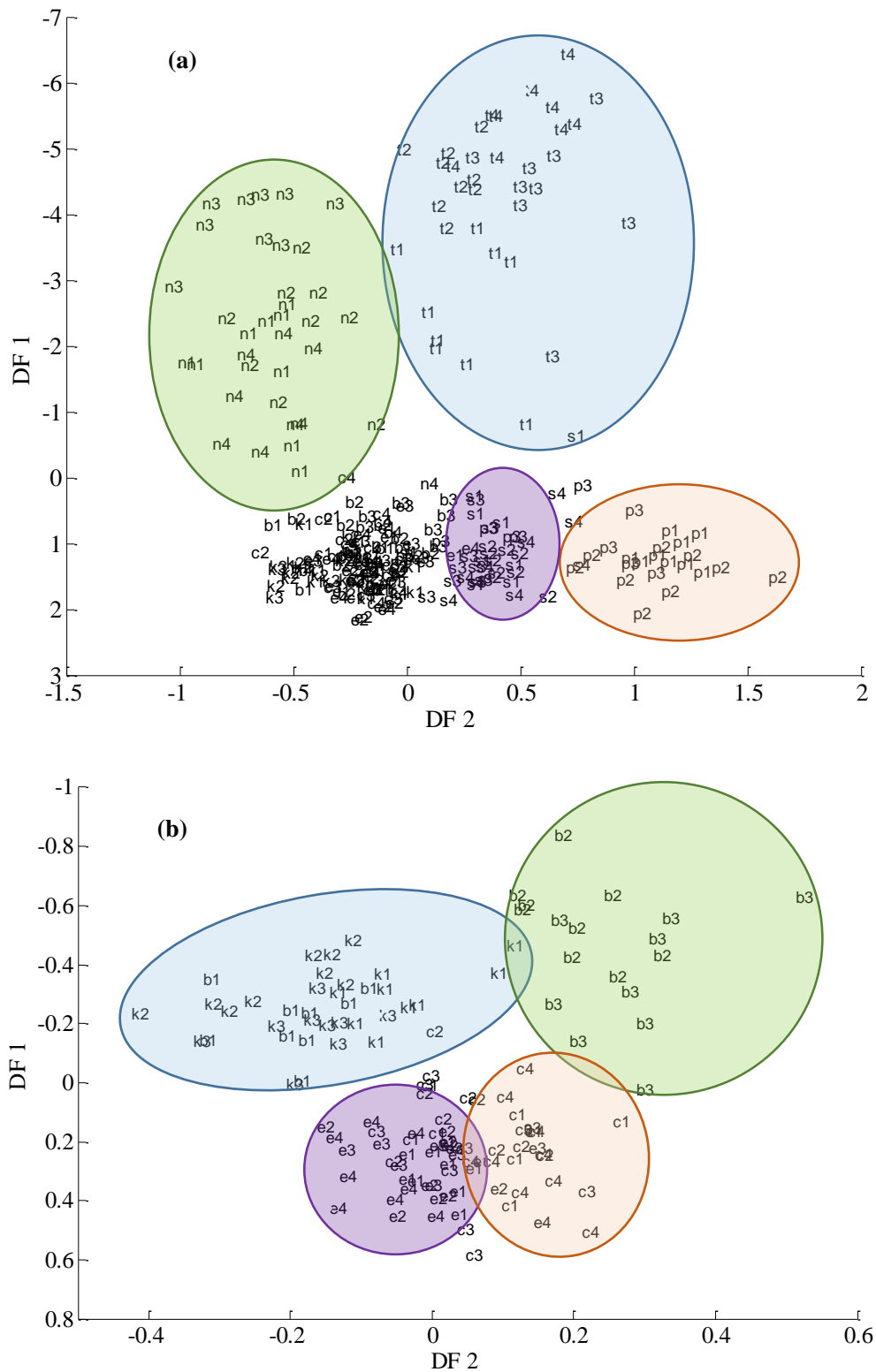


Figure 4-22. (a) DFA result of SCRS analysis from 8 species (*Citrobacter*, *E. coli*, *Enterobacter*, *Enterococcus*, *Klebsiella*, *Pseudomonas*, *S. aureus*, *Streptococcus*). (b) DFA result of SCRS analysis from 4 species (*Citrobacter*, *E. coli*, *Enterobacter*, *Klebsiella*).

4.4 Raman based Single cell isolation and gene sequencing

It has been confirmed practically that Raman activated cell ejection (RACE) can successfully isolate individual cells using a pulsed laser beam. This can be observed from cell images taken before and after ejection. A typical example is the isolation of ^{13}C -labeled cells from MNPs-free samples from environmental microbial communities (see section 4.2.1). The target cells were first measured by Raman, confirmed that they were labeled with ^{13}C according to their Raman spectra, and then accurately isolated by RACE. The comparison image before and after ejection is shown in Figure 4-23.

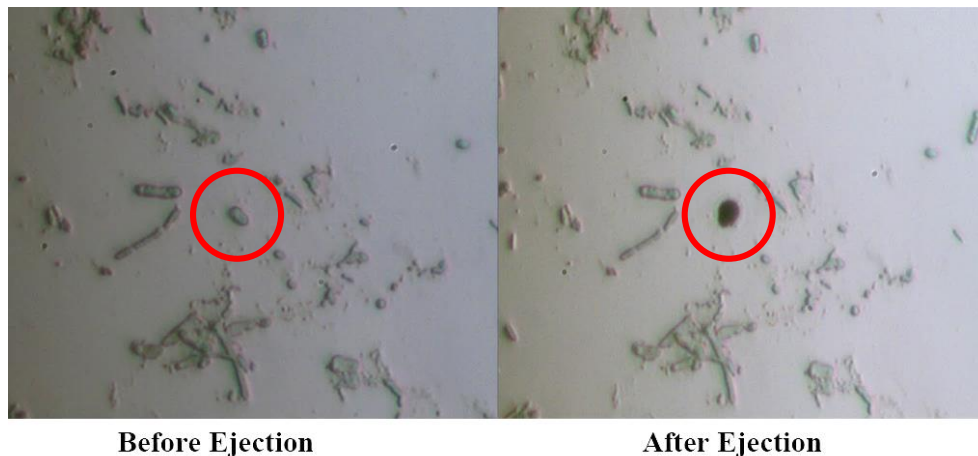


Figure 4-23. Comparison images before and after isolation of a ^{13}C -labeled MNPs-free single cell by RACE (50x zoom lens).

Several pre-experiments have been done using the single cell ejection technique to eject *Vibrio* strain AND4 bacteria, followed by DNA amplification and 16S PCR to produce DNA fragments for gene sequencing. The number of single cells in each sample varied from 5 to 50, but none of them gave the correct gene sequencing result. Two phenomena were found during these experiments. Firstly, the agarose gel electrophoresis results showed that all of the samples contained a DNA fragment after both the DNA

amplification and 16S PCR steps, including the negative controls (blank tube). Secondly, the sequencing results of all samples within one experiment were always the same (including the negative control), but gave different results for each repetition of the experiment. These phenomena indicated that the samples were somehow being contaminated by other cells (from the air, tubes, gloves, tips, etc.). Moreover, although the gene sequencing always gave results, these were merely from contamination rather than the ejected cells. Contamination can easily occur as the number of cells in each sample are so few only a few randomly introduced contaminating cells are needed to influence the results. There are two possible reasons why the sequencing results were the sequence of contaminating cells rather than ejected cells. One is that the amount of contaminated cells present were much more than the ejected cells and thus would have more opportunity to be DNA amplified. Another is that the ejected cells did not actually drop into the tubes, which means that the RACE methodology does not work. Therefore, an experiment was designed to test whether this method works or not.

The bacteria used in this study was *Pseudomonas putida* UWC1 (GFP), incubated on a LB-kanamycin (50 µg/mL) agar plate overnight then spread on the mixed membrane slide. There were a total of 6 samples containing isolated cells, specifically, around 100 cells in sample 1 and 2, 40 cells in sample 3 and 4, 10 cells in sample 5 and 6. The DNA in these 6 samples, plus a positive control (1µL of washed GFP-UWC1 cells in water) and a negative control (blank tube), were amplified using multiple displacement amplification kit (REPLI-g Single Cell Kit, Qiagen UK Ltd), which is used as a DNA template for PCR using GFP primer pairs. Figure 4-24 shows the agarose gel image following electrophoresis of the genomic DNA after PCR from 8 samples. As is shown in the image, sample 1, sample 2 and the positive control show a DNA fragment band whilst the others do not, which means samples 1 and 2 successfully contained DNA from the GFP-UWC1 cells. DNA sequencing of the fragments from these 3 samples showed them to be the gene from the GFP-UWC1 bacteria.

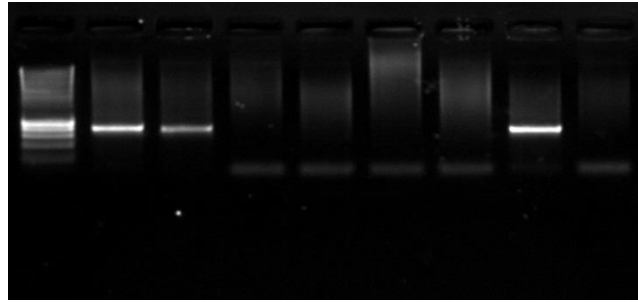


Figure 4-24. The gel image of PCR genomic DNA from 8 samples. L is a 1Kb DNA marker ladder, 1-6 are the numbers of the samples, ++ is the positive control, -- is the negative control.

This experiment not only proved that the method is workable, but also gave an answer to what quantity of cells is required (around 100) to obtain a positive result without contamination. Hence, the main challenge so far is how to prevent contamination. Several researchers have reported that true single-cell genomic sequencing is achievable (Siegl *et al.*, 2011, Gole *et al.*, 2013, Kamke *et al.*, 2013), giving us increased confidence in the success of single-cell genomics using the RACE method. However, gene sequencing from one single cell cannot be done until the contamination problem is solved.

Chapter 5: Conclusion

This study has addressed all the objectives laid out in the beginning:

- This study has demonstrated that Raman spectra contain rich biomolecular information of single cells which can be used as biomarkers to differentiate bacteria. It paves the way for Raman activated cell sorting.

It is the first time that proteorhodopsin (PR) in single cells was detected by Raman microspectroscopy and the unique band of PR can be used as a biomarker to reveal uncultured PR-containing bacteria. A paper is in preparation.

This study discovered that a new C-D (carbon-deuterium) Raman band appeared in 'silent region' when the cells incorporated deuterium from deuterated substrates (e.g. deuterated glucose). This C-D band is clear without background interference and it can be used as a universal biomarker to indicate cell metabolic activity when applied to D₂O or unravel metabolism of a deuterated compounds when applied to deuterated substrates. A PNAS paper about C-D biomarker has been submitted for reviewing.

- This research has successfully developed the Raman activated cell ejection (RACE) technique. This technique has been applied to a real environmental sample, identifying ¹³C-labeled cells and specifically isolating these targeted cells using RACE.

This is the first time that researchers can identify cells using Raman spectra and accurately isolate the targeted cells using cell ejection technology. An invited article about RACE technique has been published in Spectroscopy Europe.

- This study has contributed to reveal key but uncultured phenol degraders in wastewater from Tata Steel wastewater treatment plant and confirmed that as a group of uncultured *Burkholderiales* spp. (the identification was done by co-authors). The study has been published in ISME J recently (Zhang et al., 2014).

Chapter 6: **Proposed future works**

As discussed above, this study has carried out a large amount of experiments that have enlarged the knowledge of single-cell identification by discovering particular biomarkers, establishing the possibility of rapid sorting, linking microbial species to their functions, and distinguishing different microbial species through multivariate data analysis. These successes have laid the foundations for future single-cell isolation work. As for the section on single-cell isolation and gene sequencing, the RACE study has confirmed that cells can be successfully isolated, but subsequent DNA sequencing was hampered by the problem of cell contamination.

Based on the finished work, proposed future works should focus on the following sections:

(1) Currently, the main challenge facing the RACE technique is the presence of contaminating DNA in the single cell samples to be gene sequenced. Further work is needed to eliminate this contamination, which could be done by doing the single-cell isolation procedure in a sterile environment, pre-treating all the tubes and tips with UV light (Rinke *et al.*, 2013), wearing sterile medical gloves, etc.

(2) In order to culture the cells isolated by the RACE technique, a study should be done to test if the cells can survive following isolation. Researchers have reported the survival of population-level cells after LIFT treatment (Hopp *et al.*, 2005), but whether it works on a single cell or not still remains unknown.

(3) Optimize the RACE system to become a powerful, rapid, and easy to use tool to achieve the goal of automatic rapid screening and isolation for use in analyzing complex environmental samples.

(4) Apply the RACE technique to more real environmental samples. The complexity of environmental microbial communities will make this

experiment much more difficult than using cultured samples grown in the laboratory. This complexity will create many new challenges that will need to overcome.

The RACE technique has not proved to be successful with regard to single-cell gene sequencing in this first year study primarily because of the difficulty in reducing contamination, which will be the greatest challenge in any further research. However theoretically, this technique should be feasible, not only because a larger amount of cells (about 100) were successfully isolated and sequenced in the experiment described above, but also several references have already proved the possibility of single-cell gene sequencing. Wang and co-workers in Qingdao, China have published a paper, showing successful sequencing using almost the same method (Wang et al., 2013). With ongoing improvements towards a sterile environment, the RACE project should have had a good chance of achieving a breakthrough in the near future.

References

- AMANN, R. I., LUDWIG, W. & SCHLEIFER, K. H. 1995. Phylogenetic identification and in-situ detection of individual microbial-cells without cultivation. *Microbiological Reviews*, 59, 143-169.
- AVERY, S. V. 2006. Microbial cell individuality and the underlying sources of heterogeneity. *Nat Rev Microbiol*, 4, 577-87.
- B J , O., ARAVIND, L., KOONIN, E. V., SUZUKI, M. T., HADD, A., NGUYEN, L. P., JOVANOVIĆ, S. B., GATES, C. M., FELDMAN, R. A., SPUDICH, J. L., SPUDICH, E. N. & DELONG, E. F. 2000. Bacterial Rhodopsin: Evidence for a New Type of Phototrophy in the Sea. *Science*, 289, 1902-1906.
- BAUCHOP, T. & ELSDEN, S. R. 1960. The Growth of Micro-Organisms in Relation to Their Energy Supply. *Journal of General Microbiology*, 23, 457-469.
- BEJA, O., SPUDICH, E. N., SPUDICH, J. L., LECLERC, M. & DELONG, E. F. 2001. Proteorhodopsin phototrophy in the ocean. *Nature*, 411, 786-789.
- BELONGUER, A., DUNCAN, S. H., CALDER, A. G., HOLTROP, G., LOUIS, P., LOBLEY, G. E. & FLINT, H. J. 2006. Two routes of metabolic cross-feeding between *Bifidobacterium adolescentis* and butyrate-producing anaerobes from the human gut. *Applied And Environmental Microbiology*, 72, 3593-3599.
- BOSCHKER, H. T. S., NOLD, S. C., WELLSBURY, P., BOS, D., DE GRAAF, W., PEL, R., PARKES, R. J. & CAPPENBERG, T. E. 1998. Direct linking of microbial populations to specific biogeochemical processes by C-13-labelling of biomarkers. *Nature*, 392, 801-805.
- BREHM-STECHER, B. F. & JOHNSON, E. A. 2004. Single-cell microbiology: tools, technologies, and applications. *Microbiol Mol Biol Rev*, 68, 538-59, table of contents.
- BROWNE, W. R. & MCGARVEY, J. J. 2007. The Raman effect and its application to electronic spectroscopies in metal-centered species: Techniques and investigations in ground and excited states. *Coordination Chemistry Reviews*, 251, 454-473.
- BUCKLEY, D. H., HUANGYUTITHAM, V., HSU, S. F. & NELSON, T. A. 2007. Stable isotope probing with (15)N achieved by disentangling the effects of genome G+C content and isotope enrichment on DNA density. *Applied And Environmental Microbiology*, 73, 3189-3195.
- CADISCH, G., ESPANA, M., CAUSEY, R., RICHTER, M., SHAW, E., MORGAN, J. A. W., RAHN, C. & BENDING, G. D. 2005. Technical considerations for the use of N-15-DNA stable-isotope probing for functional microbial activity in soils. *Rapid Communications In Mass Spectrometry*, 19, 1424-1428.
- CHAN, J. W., ESPOSITO, A. P., TALLEY, C. E., HOLLARS, C. W., LANE, S. M. & HUSER, T. 2004. Reagentless identification of single bacterial spores in aqueous solution by confocal laser tweezers Raman spectroscopy. *Analytical Chemistry*, 76, 599-603.

- CHOO-SMITH, L. P., MAQUELIN, K., VAN VREESWIJK, T., BRUINING, H. A., PUPPELS, G. J., THI, N. A. G., KIRSCHNER, C., NAUMANN, D., AMI, D., VILLA, A. M., ORSINI, F., DOGLIA, S. M., LAMFARRAJ, H., SOCKALINGUM, G. D., MANFAIT, M., ALLOUCH, P. & ENDTZ, H. P. 2001. Investigating microbial (micro)colony heterogeneity by vibrational spectroscopy. *Applied And Environmental Microbiology*, 67, 1461-1469.
- DAIMS, H., NIELSEN, J. L., NIELSEN, P. H., SCHLEIFER, K. H. & WAGNER, M. 2001. In situ characterization of Nitrospira-like nitrite oxidizing bacteria active in wastewater treatment plants. *Applied And Environmental Microbiology*, 67, 5273-5284.
- DE KIEVIT, T. R., GILLIS, R., MARX, S., BROWN, C. & IGLEWSKI, B. H. 2001. Quorum-sensing genes in *Pseudomonas aeruginosa* biofilms: Their role and expression patterns. *Applied And Environmental Microbiology*, 67, 1865-1873.
- DENG, H., BLOOMFIELD, V. A., BENEVIDES, J. M. & THOMAS, G. J. 1999. Dependence of the raman signature of genomic B-DNA on nucleotide base sequence. *Biopolymers*, 50, 656-666.
- FOGARASSY, E., FUCHS, C., KERHERVE, F., HAUCHECORNE, G. & PERRIERE, J. 1989. Laser-induced forward transfer - a new approach for the deposition of high-*tc* superconducting thin-films. *Journal Of Materials Research*, 4, 1082-1086.
- GOLE, J., GORE, A., RICHARDS, A., CHIU, Y. J., FUNG, H. L., BUSHMAN, D., CHIANG, H. I., CHUN, J., LO, Y. H. & ZHANG, K. 2013. Massively parallel polymerase cloning and genome sequencing of single cells using nanoliter microwells. *Nat Biotechnol.*
- GOODACRE, R., TIMMINS, E. M., BURTON, R., KADERBHAI, N., WOODWARD, A. M., KELL, D. B. & ROONEY, P. J. 1998. Rapid identification of urinary tract infection bacteria using hyperspectral whole-organism fingerprinting and artificial neural networks. *Microbiology-Uk*, 144, 1157-1170.
- HANDELSMAN, J. 2004. Metagenomics: Application of genomics to uncultured microorganisms. *Microbiology And Molecular Biology Reviews*, 68, 669-+.
- HANDELSMAN, J., RONDON, M. R., BRADY, S. F., CLARDY, J. & GOODMAN, R. M. 1998. Molecular biological access to the chemistry of unknown soil microbes: A new frontier for natural products. *Chemistry & Biology*, 5, R245-R249.
- HARZ, A., ROSCH, P. & POPP, J. 2009. Vibrational Spectroscopy-A Powerful Tool for the Rapid Identification of Microbial Cells at the Single-Cell Level. *Cytometry Part A*, 75A, 104-113.
- HERZENBERG, L. A., PARKS, D., SAHAF, B., PEREZ, O., ROEDERER, M. & HERZENBERG, L. A. 2002. The history and future of the fluorescence activated cell sorter and flow cytometry: A view from Stanford. *Clinical Chemistry*, 48, 1819-1827.
- HERZENBERG, L. A., SWEET, R. G. & HERZENBERG, L. A. 1976. Fluorescence-activated cell sorting. *Sci Am*, 234, 108-17.

- HOPP, B., SMAUSZ, T., KRESZ, N., BARNA, N., BOR, Z., KOLOZSVARI, L., CHRISEY, D. B., SZABO, A. & NOGRADI, A. 2005. Survival and proliferative ability of various living cell types after laser-induced forward transfer. *Tissue Engineering*, 11, 1817-1823.
- HUANG, W. E., BAILEY, M. J., THOMPSON, I. P., WHITELEY, A. S. & SPIERS, A. J. 2007a. Single-cell Raman spectral profiles of *Pseudomonas fluorescens* SBW25 reflects in vitro and in planta metabolic history. *Microbial Ecology*, 53, 414-425.
- HUANG, W. E., FERGUSON, A., SINGER, A. C., LAWSON, K., THOMPSON, I. P., KALIN, R. M., LARKIN, M. J., BAILEY, M. J. & WHITELEY, A. S. 2009a. Resolving genetic functions within microbial populations: in situ analyses using rRNA and mRNA stable isotope probing coupled with single-cell raman-fluorescence in situ hybridization. *Appl Environ Microbiol*, 75, 234-41.
- HUANG, W. E., GRIFFITHS, R. I., THOMPSON, I. P., BAILEY, M. J. & WHITELEY, A. S. 2004. Raman microscopic analysis of single microbial cells. *Analytical Chemistry*, 76, 4452-4458.
- HUANG, W. E., LI, M. Q., JARVIS, R. M., GOODACRE, R. & BANWART, S. A. 2010. Shining Light on the Microbial World: The Application of Raman Microspectroscopy. In: LASKIN, A. I., SARIASLANI, S. & GADD, G. M. (eds.) *Advances In Applied Microbiology, Vol 70*. San Diego: Elsevier Academic Press Inc.
- HUANG, W. E., STOECKER, K., GRIFFITHS, R., NEWBOLD, L., DAIMS, H., WHITELEY, A. S. & WAGNER, M. 2007b. Raman-FISH: combining stable-isotope Raman spectroscopy and fluorescence in situ hybridization for the single cell analysis of identity and function. *Environ Microbiol*, 9, 1878-89.
- HUANG, W. E., UDE, S. & SPIERS, A. J. 2007c. *Pseudomonas fluorescens* SBW25 biofilm and planktonic cells have differentiable Raman spectral profiles. *Microbial Ecology*, 53, 471-474.
- HUANG, W. E., WARD, A. D. & WHITELEY, A. S. 2009b. Raman tweezers sorting of single microbial cells. *Environ Microbiol Rep*, 1, 44-9.
- JARVIS, R. M., BROOKER, A. & GOODACRE, R. 2004. Surface-enhanced Raman spectroscopy for bacterial discrimination utilizing a scanning electron microscope with a Raman spectroscopy interface. *Analytical Chemistry*, 76, 5198-5202.
- KAERN, M., ELSTON, T. C., BLAKE, W. J. & COLLINS, J. J. 2005. Stochasticity in gene expression: From theories to phenotypes. *Nature Reviews Genetics*, 6, 451-464.
- KAMKE, J., SCZYRBA, A., IVANOVA, N., SCHWIENTEK, P., RINKE, C., MAVROMATIS, K., WOYKE, T. & HENTSCHER, U. 2013. Single-cell genomics reveals complex carbohydrate degradation patterns in poribacterial symbionts of marine sponges. *ISME J*, 7, 2287-300.
- KNEIPP, J., KNEIPP, H., MCLAUGHLIN, M., BROWN, D. & KNEIPP, K. 2006. In vivo molecular probing of cellular compartments with gold nanoparticles and nanoaggregates. *Nano Letters*, 6, 2225-2231.

- KOPKE, B., WILMS, R., ENGELEN, B., CYPIONKA, H. & SASS, H. 2005. Microbial diversity in coastal subsurface sediments: a cultivation approach using various electron acceptors and substrate gradients. *Applied And Environmental Microbiology*, 71, 7819-7830.
- LEE, N., NIELSEN, P. H., ANDREASEN, K. H., JURETSCHKO, S., NIELSEN, J. L., SCHLEIFER, K. H. & WAGNER, M. 1999. Combination of fluorescent in situ hybridization and microautoradiography - a new tool for structure-function analyses in microbial ecology. *Applied And Environmental Microbiology*, 65, 1289-1297.
- LI, M., CANNIFFE, D. P., JACKSON, P. J., DAVISON, P. A., FITZGERALD, S., DICKMAN, M. J., BURGESS, J. G., HUNTER, C. N. & HUANG, W. E. 2012. Rapid resonance Raman microspectroscopy to probe carbon dioxide fixation by single cells in microbial communities. *ISME J*, 6, 875-85.
- LI, M. Q., HUANG, W. E., GIBSON, C. M., FOWLER, P. W. & JOUSSET, A. 2013. Stable Isotope Probing and Raman Spectroscopy for Monitoring Carbon Flow in a Food Chain and Revealing Metabolic Pathway. *Analytical Chemistry*, 85, 1642-1649.
- LONG, D. A. 2002. *The Raman Effect: A Unified Treatment of the Theory of Raman Scattering by Molecules*, Wiley.
- MANEFIELD, M., WHITELEY, A. S., GRIFFITHS, R. I. & BAILEY, M. J. 2002a. RNA Stable Isotope Probing, a Novel Means of Linking Microbial Community Function to Phylogeny. *Applied and Environmental Microbiology*, 68, 5367-5373.
- MANEFIELD, M., WHITELEY, A. S., OSTLE, N., INESON, P. & BAILEY, M. J. 2002b. Technical considerations for RNA-based stable isotope probing: an approach to associating microbial diversity with microbial community function. *Rapid Communications In Mass Spectrometry*, 16, 2179-2183.
- MANLY, B. F. J. 1994. *Multivariate Statistical Methods: A Primer, Second Edition*, Taylor & Francis.
- MAQUELIN, K., CHOO-SMITH, L. P., ENDTZ, H. P., BRUINING, H. A. & PUPPELS, G. J. 2002a. Rapid identification of *Candida* species by confocal Raman micro spectroscopy. *Journal Of Clinical Microbiology*, 40, 594-600.
- MAQUELIN, K., CHOO-SMITH, L. P., VAN VREESWIJK, T., ENDTZ, H. P., SMITH, B., BENNETT, R., BRUINING, H. A. & PUPPELS, G. J. 2000. Raman spectroscopic method for identification of clinically relevant microorganisms growing on solid culture medium. *Analytical Chemistry*, 72, 12-19.
- MAQUELIN, K., DIJKSHOORN, L., VAN DER REIJDEN, T. J. K. & PUPPELS, G. J. 2006. Rapid epidemiological analysis of *Acinetobacter* strains by Raman spectroscopy. *Journal Of Microbiological Methods*, 64, 126-131.
- MAQUELIN, K., KIRSCHNER, C., CHOO-SMITH, L. P., VAN DEN BRAAK, N., ENDTZ, H. P., NAUMANN, D. & PUPPELS, G. J. 2002b. Identification of medically relevant microorganisms by

- vibrational spectroscopy. *Journal Of Microbiological Methods*, 51, 255-271.
- MARCHESE, J. R., SATO, T., WEIGHTMAN, A. J., MARTIN, T. A., FRY, J. C., HIOM, S. J. & WADE, W. G. 1998. Design and evaluation of useful bacterium-specific PCR primers that amplify genes coding for bacterial 16S rRNA. *Applied and Environmental Microbiology*, 64, 795-799.
- MIKX, F. H. M. & VANDERHOEVEN, J. S. 1975. SYMBIOSIS OF STREPTOCOCCUS-MUTANS AND VEILLONELLA-ALCALESCENS IN MIXED CONTINUOUS CULTURES. *Archives Of Oral Biology*, 20, 407-410.
- MURRAY, G. I. 2007. An overview of laser microdissection technologies. *Acta Histochemica*, 109, 171-176.
- NEUFELD, J. D., VOHRA, J., DUMONT, M. G., LUEDERS, T., MANEFIELD, M., FRIEDRICH, M. W. & MURRELL, J. C. 2007. DNA stable-isotope probing. *Nat Protoc*, 2, 860-6.
- OKADA, M., SMITH, N. I., PALONPON, A. F., ENDO, H., KAWATA, S., SODEOKA, M. & FUJITA, K. 2012. Label-free Raman observation of cytochrome c dynamics during apoptosis. *Proceedings of the National Academy of Sciences*, 109, 28-32.
- OUVERNEY, C. C. & FUHRMAN, J. A. 1999. Combined Microautoradiography-16S rRNA probe technique for determination of radioisotope uptake by specific microbial cell types in situ. *Applied And Environmental Microbiology*, 65, 1746-1752.
- PUPPELS, G. J., DE MUL, F. F., OTTO, C., GREVE, J., ROBERT-NICOUD, M., ARNDT-JOVIN, D. J. & JOVIN, T. M. 1990. Studying single living cells and chromosomes by confocal Raman microspectroscopy. *Nature*, 347, 301-3.
- RADAJEWSKI, S., INESON, P., PAREKH, N. R. & MURRELL, J. C. 2000. Stable-isotope probing as a tool in microbial ecology. *Nature*, 403, 646-649.
- RAMAN, C. V. & KRISHNAN, K. S. 1928. A New Type of Secondary Radiation. *Nature*, 121, 501-502.
- RINKE, C., SCHWIENSTEK, P., SCZYRBA, A., IVANOVA, N. N., ANDERSON, I. J., CHENG, J. F., DARLING, A., MALFATTI, S., SWAN, B. K., GIES, E. A., DODSWORTH, J. A., HEDLUND, B. P., TSIAMIS, G., SIEVERT, S. M., LIU, W. T., EISEN, J. A., HALLAM, S. J., KYRPIDES, N. C., STEPANAUSKAS, R., RUBIN, E. M., HUGENHOLTZ, P. & WOYKE, T. 2013. Insights into the phylogeny and coding potential of microbial dark matter. *Nature*, 499, 431-7.
- ROSCH, P., HARZ, M., SCHMITT, M., PESCHKE, K. D., RONNEBERGER, O., BURKHARDT, H., MOTZKUS, H. W., LANKERS, M., HOFER, S., THIELE, H. & POPP, J. 2005. Chemotaxonomic identification of single bacteria by micro-Raman spectroscopy: Application to clean-room-relevant biological contaminations. *Applied And Environmental Microbiology*, 71, 1626-1637.

- ROSCH, P., SCHNEIDER, H., ZIMMERMANN, U., KIEFER, W. & POPP, J. 2004. In situ Raman investigation of single lipid droplets in the water-conducting xylem of four woody plant species. *Biopolymers*, 74, 151-156.
- SCHENZEL, K. & FISCHER, S. 2001. NIR FT Raman spectroscopy - a rapid analytical tool for detecting the transformation of cellulose polymorphs. *Cellulose*, 8, 49-57.
- SCHULTZE, V. & WAGNER, M. 1991. Laser-induced forward transfer of aluminum. *Applied Surface Science*, 52, 303-309.
- SCHUSTER, K. C., REESE, I., URLAUB, E., GAPES, J. R. & LENDL, B. 2000a. Multidimensional information on the chemical composition of single bacterial cells by confocal Raman microspectroscopy. *Analytical Chemistry*, 72, 5529-5534.
- SCHUSTER, K. C., URLAUB, E. & GAPES, J. R. 2000b. Single-cell analysis of bacteria by Raman microscopy: spectral information on the chemical composition of cells and on the heterogeneity in a culture. *Journal of Microbiological Methods*, 42, 29-38.
- SCHWARTZ, E. 2007. Characterization of growing microorganisms in soil by stable isotope probing with (H₂O)-O-18. *Applied And Environmental Microbiology*, 73, 2541-2546.
- SIEGL, A., KAMKE, J., HOCHMUTH, T., PIEL, J., RICHTER, M., LIANG, C., DANDEKAR, T. & HENTSCHEL, U. 2011. Single-cell genomics reveals the lifestyle of Poribacteria, a candidate phylum symbiotically associated with marine sponges. *ISME J*, 5, 61-70.
- SMITH, E. & DENT, G. 2005. *Modern Raman Spectroscopy: A Practical Approach*, Wiley.
- STREIT, W. R., DANIEL, R. & JAEGER, K. E. 2004. Prospecting for biocatalysts and drugs in the genomes of non-cultured microorganisms. *Current Opinion In Biotechnology*, 15, 285-290.
- TAKAI, Y., MASUKO, T. & TAKEUCHI, H. 1997. Lipid structure of cytotoxic granules in living human killer T lymphocytes studied by Raman microspectroscopy. *Biochimica Et Biophysica Acta-General Subjects*, 1335, 199-208.
- TAMAKI, H., SEKIGUCHI, Y., HANADA, S., NAKAMURA, K., NOMURA, N., MATSUMURA, M. & KAMAGATA, Y. 2005. Comparative analysis of bacterial diversity in freshwater sediment of a shallow eutrophic lake by molecular and improved cultivation-based techniques. *Applied And Environmental Microbiology*, 71, 2162-2169.
- TSAI, Y. L. & OLSON, B. H. 1992. Rapid method for separation of bacterial-DNA from humic substances in sediments for polymerase chain-reaction. *Applied And Environmental Microbiology*, 58, 2292-2295.
- TYSON, G. W., CHAPMAN, J., HUGENHOLTZ, P., ALLEN, E. E., RAM, R. J., RICHARDSON, P. M., SOLOVYEV, V. V., RUBIN, E. M., ROKHSAR, D. S. & BANFIELD, J. F. 2004. Community structure and metabolism through reconstruction of microbial genomes from the environment. *Nature*, 428, 37-43.
- UZUNBAJAKAVA, N., LENFERINK, A., KRAAN, Y., VOLOKHINA, E., VRENSSEN, G., GREVE, J. & OTTO, C. 2003a. Nonresonant

- confocal Raman imaging of DNA and protein distribution in apoptotic cells. *Biophysical Journal*, 84, 3968-3981.
- UZUNBAJAKAVA, N., LENFERINK, A., KRAAN, Y., WILLEKENS, B., VRENSSEN, G., GREVE, J. & OTTO, C. 2003b. Nonresonant Raman imaging of protein distribution in single human cells. *Biopolymers*, 72, 1-9.
- VAN MANEN, H. J., KRAAN, Y. M., ROOS, D. & OTTO, C. 2005. Single-cell Raman and fluorescence microscopy reveal the association of lipid bodies with phagosomes in leukocytes. *Proceedings Of the National Academy Of Sciences Of the United States Of America*, 102, 10159-10164.
- VENTER, J. C., REMINGTON, K., HEIDELBERG, J. F., HALPERN, A. L., RUSCH, D., EISEN, J. A., WU, D. Y., PAULSEN, I., NELSON, K. E., NELSON, W., FOUTS, D. E., LEVY, S., KNAP, A. H., LOMAS, M. W., NEALSON, K., WHITE, O., PETERSON, J., HOFFMAN, J., PARSONS, R., BADEN-TILLSON, H., PFANNKOCHE, C., ROGERS, Y. H. & SMITH, H. O. 2004. Environmental genome shotgun sequencing of the Sargasso Sea. *Science*, 304, 66-74.
- WANG, Y., JI, Y., WHARFE, E. S., MEADOWS, R. S., MARCH, P., GOODACRE, R., XU, J. & HUANG, W. E. 2013. Raman activated cell ejection for isolation of single cells. *Analytical chemistry*, 85, 10697-701.
- WHITEHEAD, N. A., BARNARD, A. M. L., SLATER, H., SIMPSON, N. J. L. & SALMOND, G. P. C. 2001. Quorum-sensing in gram-negative bacteria. *Fems Microbiology Reviews*, 25, 365-404.
- WHITMAN, W. B., COLEMAN, D. C. & WIEBE, W. J. 1998. Prokaryotes: The unseen majority. *Proceedings Of the National Academy Of Sciences Of the United States Of America*, 95, 6578-6583.
- XIE, C., CHEN, D. & LI, Y. Q. 2005a. Raman sorting and identification of single living micro-organisms with optical tweezers. *Opt Lett*, 30, 1800-2.
- XIE, C. & LI, Y.-Q. 2002. Raman spectra and optical trapping of highly refractive and nontransparent particles. *Applied Physics Letters*, 81, 951-953.
- XIE, C., MACE, J., DINNO, M. A., LI, Y. Q., TANG, W., NEWTON, R. J. & GEMPERLINE, P. J. 2005b. Identification of single bacterial cells in aqueous solution using confocal laser tweezers Raman spectroscopy. *Analytical Chemistry*, 77, 4390-4397.
- XIE, C. G. & LI, Y. Q. 2003. Confocal micro-Raman spectroscopy of single biological cells using optical trapping and shifted excitation difference techniques. *Journal Of Applied Physics*, 93, 2982-2986.
- ZHANG, D., BERRY, J. P., ZHU, D., WANG, Y., CHEN, Y., JIANG, B., HUANG, S., LANGFORD, H., LI, G., DAVISON, P. A., XU, J., ARIES, E. & HUANG, W. E. 2014. Magnetic nanoparticle-mediated isolation of functional bacteria in a complex microbial community. *ISME J.*

Appendix

Appendix 1. Assignment of some bands frequently occurred in single cell Raman spectra

Frequency (cm ⁻¹)	Assignment	Reference
3240	water	(Harz <i>et al.</i> , 2009)
3059	(C=C-H) aromatic str	(Maquelin <i>et al.</i> , 2002b)
2975	CH ₃ str	(Maquelin <i>et al.</i> , 2002b)
2935	C-H str,	(Harz <i>et al.</i> , 2009, Maquelin <i>et al.</i> , 2002b)
2870-2890	CH ₂ str	(Maquelin <i>et al.</i> , 2002b)
1735	>C=O ester str	(Maquelin <i>et al.</i> , 2002b)
1650-1680	Amide I	(Maquelin <i>et al.</i> , 2002b)
1663	Amide I	
1658	Unsaturated lipids	(van Manen <i>et al.</i> , 2005)
1614	Tyrosine	(Maquelin <i>et al.</i> , 2002b)
1605-1606	Phenylalanine	(Maquelin <i>et al.</i> , 2002b)
1582, 1593	Protein	(Maquelin <i>et al.</i> , 2002b, Kneipp <i>et al.</i> , 2006)
1575-1578	Guanine, Adenine (ring str)	(Maquelin <i>et al.</i> , 2002b)
1573	C=C, N-H def and C-N str (amide II)	(Schuster <i>et al.</i> , 2000a)
1516	C=C str, of sarcinaxanthin	(Rosch <i>et al.</i> , 2005)
1510	Adenine, or C=C str, carotenoids	(Uzunbajakava <i>et al.</i> , 2003b)
1505,1518,1532,1578	Adenine, Cytosine, Guanine	(Uzunbajakava <i>et al.</i> , 2003b)
1482-1487	Nucleic acids	(Schuster <i>et al.</i> , 2000b)
1441	lipids	(van Manen <i>et al.</i> , 2005)
1440-1460	C-H ₂ def	(Maquelin <i>et al.</i> , 2002b)
1431-1481	Protein marker band 1451	(Uzunbajakava <i>et al.</i> , 2003a)
1421-1427	Adenine, Guanine	(Uzunbajakava <i>et al.</i> , 2003b, Kneipp <i>et al.</i> , 2006)

1375	Thymine, Adenine, Guanine	(Uzunbajakava <i>et al.</i> , 2003b)
1336-1339	Adenine, Guanine, tyrosine, tryptophan	(Harz <i>et al.</i> , 2009, Uzunbajakava <i>et al.</i> , 2003b)
~1320	Amide III, C-H def	(Schuster <i>et al.</i> , 2000a)
1304	Adenine, amideIII	(Uzunbajakava <i>et al.</i> , 2003b)
1295	CH ₂ def	(Maquelin <i>et al.</i> , 2002b)
1214, 1240, 1254	Thymine, Cytosine, Adenine, ring v	(Uzunbajakava <i>et al.</i> , 2003b)
1254	Adenine, amideIII	(Uzunbajakava <i>et al.</i> , 2003b)
1220-1290	Amide III random, lipids	(Schuster <i>et al.</i> , 2000a)
1267	lipids	(van Manen <i>et al.</i> , 2005)
1209	Tyrosine, Phenylalanine, protein, amideIII	(Uzunbajakava <i>et al.</i> , 2003b)
1175	Tyrosine, Phenylalanine	(Uzunbajakava <i>et al.</i> , 2003b)
1155-1157	C-C str, of sarcinaxanthin, carotnoids	(Rosch <i>et al.</i> , 2005)
1154	v(CC, CN), ρ(CH ₃)	(Maquelin <i>et al.</i> , 2002b)
1145-1160	C-C, C-O ring breath, assym	(Rosch <i>et al.</i> , 2004, Schenzel and Fischer, 2001)
~1130	=C-C= (unsaturated fatty acids in lipids)	(Schuster <i>et al.</i> , 2000a)
1102	>PO ₂ ⁻ str (sym)	(Maquelin <i>et al.</i> , 2002b)
1100	Glass background	(Schuster <i>et al.</i> , 2000a)
1098-1099	Phosphate, CC skeletal and COC str from glycosidic link	(Maquelin <i>et al.</i> , 2002b)
1085	C-O str	(Maquelin <i>et al.</i> , 2002b)
1061	C-N and C-C str	(Maquelin <i>et al.</i> , 2002b)
1054	Nucleic acids, CO str; protein, C-N str	(Uzunbajakava <i>et al.</i> , 2003b)

1032	Phenylalanine; C-N str	(Uzunbajakava <i>et al.</i> , 2003b)
1030-1130	Carbohydrates, mainly –C-C- (skeletal), C-O, def (C-O-H)	(Schuster <i>et al.</i> , 2000a)
~1004	Phenylalanine, substituted benzene derivatives	(Maquelin <i>et al.</i> , 2002b)
897	COC str	(Maquelin <i>et al.</i> , 2002b)
858	CC str, COC 1,4 glycosidic link	(Maquelin <i>et al.</i> , 2002b)
~850	Buried tyrosine	(Maquelin <i>et al.</i> , 2002b)
~830	Exposed tyrosine	(Maquelin <i>et al.</i> , 2002b)
838	DNA	(Deng <i>et al.</i> , 1999)
813	A-type helices in RNA	(Uzunbajakava <i>et al.</i> , 2003a)
810-820	Nucleic acids (C-O-P-O-C in RNA backbone)	(Schuster <i>et al.</i> , 2000a)
778-785, 792	Cytosine, uracil (ring, str)	(Maquelin <i>et al.</i> , 2002b) (Uzunbajakava <i>et al.</i> , 2003b)
748-751	O-P-O sym str	(Takai <i>et al.</i> , 1997)
752	T ring str	(Uzunbajakava <i>et al.</i> , 2003b)
730	A ring str	(Uzunbajakava <i>et al.</i> , 2003b)
720	Adenine	(Maquelin <i>et al.</i> , 2002b)
665	Guanine	(Maquelin <i>et al.</i> , 2002b)
640	Tyrosine (skeletal)	(Maquelin <i>et al.</i> , 2002b)
620	Phenylalanine (skeletal)	(Maquelin <i>et al.</i> , 2002b)
550 range	Glass background	(Schuster <i>et al.</i> , 2000a)
540	COC glycosidic ring def	(Maquelin <i>et al.</i> , 2002b)
520-540	S-S str	(Maquelin <i>et al.</i> , 2002b)
481	Skeletal modes of carbohydrates (starch)	(Schuster <i>et al.</i> , 2000a)
407	Skeletal modes of carbohydrates (glucose)	(Schuster <i>et al.</i> , 2000a)

Note: str = stretching; def = deformation; sym = symmetric; asym = antisymmetric.

Appendix 2. Recipe of minimal medium (MM) (1 L)

Minimal medium (MM) recipe (1 L):

Na₂HPO₄: 2.5 g,

KH₂PO₄: 2.5 g,

NH₄Cl: 1.0 g,

MgSO₄ · 7H₂O: 0.1 g,

Saturated CaCl₂ solution: 10 µL,

Saturated FeSO₄ solution: 10 µL,

Bauchop & Elsdén solution 1 mL (Bauchop and Elsdén, 1960).

Bauchop & Elsdén solution recipe (1 L):

MgSO₄: 10.75 g,

FeSO₄ · 7H₂O: 4.5 g,

CaCO₃: 2.0 g,

ZnSO₄ · 7H₂O: 1.44 g,

MnSO₄ · 4H₂O: 1.12 g,

CuSO₄ · 5H₂O: 0.25 g,

CoSO₄ · 7H₂O: 0.28 g,

H₃BO₃: 0.06 g,

Concentrated HCl: 51.3 mL.

Appendix 3. Recipe of M9 minimal medium (1 L)

$\text{Na}_2\text{HPO}_4 \cdot 7\text{H}_2\text{O}$: 12.8g

or

Na_2HPO_4 (anhydrous): 6 g

KH_2PO_4 : 3 g

NaCl : 0.5 g

NH_4Cl : 1 g

-Add fully-deuterated glucose to 10 mM final concentration;

-pH to 7.4 with NaOH ;

-Autoclave and then add sterile micronutrient components to a final concentration of:

Micronutrient	Final Concentration
MgSO_4	1 mM
CaCl_2	100 μM
$(\text{NH}_4)_6\text{Mo}_7\text{O}_{24} \cdot 4\text{H}_2\text{O}$	3×10^{-9} M
H_3BO_3	4×10^{-7} M
$\text{CoCl}_2 \cdot 6\text{H}_2\text{O}$	3×10^{-8} M
$\text{CuSO}_4 \cdot 5\text{H}_2\text{O}$	1×10^{-8} M
$\text{MnCl}_2 \cdot 4\text{H}_2\text{O}$	8×10^{-8} M
$\text{ZnSO}_4 \cdot 7\text{H}_2\text{O}$	1×10^{-8} M
$\text{FeSO}_4 \cdot 7\text{H}_2\text{O}$	1×10^{-6} M

Appendix 4. Recipe of $1 \times \text{M22}$ medium (2 L)

1 × M22 medium:

Make up to 2 litres

10 × M22 stock	200 ml
Casamino acids (CAA)	40 ml
water	1760 ml

10 × M22 Stock:

To make 4 litres

Potassium dihydrogen orthophosphate	KH_2PO_4	122.4 g
Dipotassium hydrogen orthophosphate	K_2HPO_4	120.0 g
DL – Lactic acid (fridge)	Na lactate solution	100.0 g
Ammonium sulphate	$(\text{NH}_4)_2\text{SO}_4$	20 g
Sodium chloride	NaCl	20 g
Sodium succinate		173.7 g
Sodium glutamate	L – Glutamic acid	10.8 g
Aspartic acid	DL – Aspartic acid	1.6 g
Solution C		800ml

Make up to 2-3 litres, pH to 6.8 and then top it up to 4 litres.

Autoclave as 10 × 400ml.

Solution C:

To make 4 litres

Nitrilotriacetic acid		40 g
Magnesium chloride	MgCl_2	96 g
Calcium chloride	CaCl_2	13.36 g
EDTA		0.5 g

Zinc chloride	ZnCl ₂	1.044 g
Ferrous chloride	FeCl ₂	1.0 g
Manganese chloride	MnCl ₂	0.36 g
Ammonium heptamolybdate	(NH ₄) ₆ Mo ₇ O ₂₄ (H ₂ O) ₄	0.037 g
Cupric chloride	CuCl ₂	0.031 g
Cobaltous nitrate	Co(NO ₃) ₂	0.0496 g
Boric acid (orthoboric acid)		0.0228 g

Do not autoclave, just freeze at -20°C in 400ml aliquots.

Casamino acids (CAA):

	To make 1 litre
Casein Hydrosylate acid	50 g

Makes up 5% solution to be aliquoted into 200ml.

Vitamins:

	1 000 ×	10 000 ×
Nicotinic acid (poison)	100 mg	1 g
Thiamine (poison)	50 mg	0.5 g
pABA (4-aminobenzoic acid) (fridge)	10 mg	0.1 g
Biotin (d-Biotin) (fridge)	1 mg	10 mg
water	100 ml	100 ml

Filter sterilise thru 0.2 µm filter. Dispense into aliquots, date and freeze. Keep working stock in the fridge.

Appendix 5. PCR reaction solution (50 µL) and program

PCR reaction solution (50 µL):

Item	Volume (µL)
------	-------------

dH ₂ O	38.5
PCR buffer (Fermentas) × 10	5
dNTPs (Sigma), 5mM	2
Forward primer (Appendix 6), 5 μM	2
Reverse primer (Appendix 6), 5 μM	2
colony/DNA	0.2
Taq polymerase (Sigma)	0.3
Total	50

PCR program:

1. 95 °C, 5 min
2. 95 °C, 1 min
3. 55 °C, 1 min
4. 72 °C, 1.5 min
5. 2-4 step, 35 cycles
6. 72 °C, 5 min
7. 12 °C, for ever

Appendix 6. Primers used in PCR

Name	Sequence	Reference
63f	CAGGCCTAACACATGCAAGTC	(Marchesi <i>et al.</i> , 1998)
1387r	GGGCGGWGTGTACAAGGC	(Marchesi <i>et al.</i> , 1998)
GFP_ADPI_for	TTAGATCTTGAGCGGATAACAATTACTAG	
GFP_ADPI_rev1	TGGAATTCGCAGCGGCCGCTACTAGTA	

Appendix 7. Gel solution of agarose gel electrophoresis

1 × TAE buffer: 100 mL (for 50 × TAE buffer, see Appendix 8),

Agarose: 1 g,

Ethidium bromide: 1 μ L

Appendix 8. 50 \times TAE stock solution (1 L)

Tris-base: 242 g,

Acetic acid: 57.1 mL,

0.5 M EDTA (pH 8.0): 100 mL,

Fill dH₂O to 1 L.